Shortening and extrusion in the East Anatolian Plateau: how was Neogene Arabia-Eurasia convergence tectonically accommodated?

Douwe J.J. van Hinsbergen[1*], Derya Gürer[2,3], Ayten Koç[4], Nalan Lom[1,2]

1. Department of Earth Sciences, Utrecht University, Budapestlaan 4, 3584 CD Utrecht, the Netherlands
2. Institute of Earth Sciences, Heidelberg University, Heidelberg, 69120, Germany
3. Research School of Earth Sciences, Australian National University, Canberra, ACT 2601, Australia
4. Department of Geological Engineering, Van Yüzüncü Yıl University, Van, Turkey

*Corresponding author: d.j.j.vanhinsbergen@uu.nl

This is a peer reviewed manuscript, accepted for publication in Earth and Planetary Science Letters

Abstract

Deformation in orogenic belts is typically widely distributed but may be localized to form discrete, fast-moving fault zones enclosing semi-rigid microplates. An example is the Anatolian microplate, which is extruding westwards from the East Anatolian Plateau in the Arabia-Eurasia collision zone along the North and East Anatolian Faults that cause devastating earthquakes, including the February 6, 2023 Southeast Anatolian earthquakes. Here, we summarize the orogenic architecture of the east Anatolian Plateau and its kinematic history since the Cretaceous, and use this to reconstruct the tectonic situation that existed at the onset of and during the development of the Neogene East Anatolian Plateau and the Anatolian microplate. The orogen first formed in the late Cretaceous by subduction-accretion of microcontinental lithosphere below Neotethys oceanic lithosphere. Then, in Paleogene time, the accretionary orogen underwent regional upper plate extension, causing crystalline crust exhumation and deep-marine basin formation. From early Miocene time onwards, the extended orogen shortened again must have accommodated ~350 km of convergence, making crust up to 45 km thick, and causing >2 km of uplift. Since the ~13 Ma onset of North Anatolian Fault formation, microplate extrusion absorbed no more than (~65 km) of Arabia-Eurasia convergence and even during this time alone, >200 km of convergence must thus have been accommodated by continued ~N-S shortening. We highlight the need for field studies of the East Anatolian Plateau to identify where and how this major shortening was accommodated, what role it played in plateau rise and the onset and dynamics of microplate extrusion, and to better assess seismic hazards.

1. Introduction

If tectonic plates were entirely rigid, as classic plate tectonic theory describes (McKenzie and Parker, 1967), seismicity would be strictly focused at discrete plate boundaries. In reality, particularly convergent plate boundaries are associated with deforming plate boundary zones formed by orogenic belts that distribute deformation over wide areas (e.g., Şengör, 1990; van Hinsbergen and Schouten, 2021). However, within such regionally deforming belts, plate boundary-like, discrete fault zones may develop that enclose semi-rigid (micro)plates (Li et al., 2017; Mann et al., 1995; Molnar and Tapponnier, 1975; Whitney et al., 2023). These fault zones are well-studied because they pose a major seismic hazard, but they may also distract attention from the regionally distributed deformation and associated hazards that surround the developing microplate formation.

The Arabia-Eurasia collision zone in eastern Anatolia is a key example of regionally distributed deformation, including microplate formation. An Anatolian 'microplate' is identified as an internally more or less rigid block bounded from Eurasia and Arabia by the North and East Anatolian transform faults, respectively, which accommodate Anatolian extrusion away from the Arabia-Eurasia collision zone (Dewey and Şengör, 1979; Ketin, 1948) (Figure 1). This motion is associated with devastating earthquakes, including the M_w 7.8 Pazarcık (Nurdağ) and M_w 7.7 Ekinözü earthquakes of February 6, 2023, at the East Anatolian Fault Zone (Barbot et al., 2023; Liu et al., 2023; Melgar et al., 2023; Zhang et al., 2023). GPS measurements show that these microplate-bounding faults accommodate much of the present-day convergence of Arabia with Eurasia (Reilinger et al., 2006). However, maps of active faults (Emre et al., 2018) reveal widespread and distributed deformation to the east and within the microplate, across faults with isolated surface ruptures that do not make a coherent fault mosaic. The earthquakes of 2023 placed understanding the dynamics of eastern Anatolian deformation once again at the focus of scientific attention. Whereas the extrusion-accommodating 'microplate boundaries' receive – logically – most attention, we here focus on the possible role that distributed deformation may have on adding seismic hazard and what information it may hold about microplate evolution and dynamics.

In this paper, we first summarize the orogenic evolution of the East Anatolian Orogen since the Late Cretaceous that preconditioned plateau rise and microplate formation in the Miocene, based on a recent detailed regional kinematic restoration of Mediterranean tectonics (van Hinsbergen et al., 2020). We then explain the underlying structural geological and paleomagnetic data that allow the reconstruction of microplate formation and motion. Next, we estimate the amount of shortening that must have occurred during microplate development since 13 Ma by comparing the amount of convergence accommodated by Anatolian extrusion with the documented amount of Arabia-Eurasia plate convergence. We then evaluate how and where the remaining convergence may have been accommodated and what role shortening may have played in driving the initiation and evolution of East Anatolian Plateau rise, microplate formation, and extrusion. Finally, we identify targets for future field research to aid seismic hazard assessment associated with distributed deformation in the east Anatolian orogenic belt that occurs outside of the major North and East Anatolian transform faults.

2. Regional plate tectonic setting and subduction history

The Anatolian orogen formed due to continental and oceanic subduction at multiple subduction plate boundaries that accommodated convergence between Africa-Arabia and Eurasia since the Mesozoic. The North and East Anatolian faults, which delineate the modern Anatolian microplate, are relatively young structures that cut through this older orogenic belt (Figure 2). Here, we summarize the history of subduction and orogenesis for the eastern Anatolian part of the system. For a more detailed account of the plate kinematic setting, orogenic architecture, and regional context of Mediterranean tectonics, we refer the reader to van Hinsbergen et al. (2020).

The eastern Anatolian orogen is often referred to as the East Anatolian Plateau and represents the topographically highest part of the mountain belt, with a modern average elevation of 2 km and peaks well over 3 km. It is supported by crust that is up to 45 km thick, and a mantle lithosphere that is in many places thinner than 100 km (Barazangi et al., 2006; Zor et al., 2003; Artemieva and Shulgin, 2019). This plateau is widely covered by young volcanics (Keskin, 2003), but below these, crystalline and non-crystalline nappes, ophiolites, plutons, and Cenozoic sedimentary basins and volcanics are exposed that allow correlation to better-exposed and better-studied orogenic architecture to the west (Figure 3).

The Pontides-Lesser Caucasus fold-thrust belt of northern Turkey, Armenia and Azerbaijan consists of continental fragments that collided with Eurasia in or prior to the Late Jurassic, forming the southern active margin of Eurasia since then. It was located above a north-dipping subduction zone, south of associated back-arc basins (Şengör and Yılmaz, 1981; van Hinsbergen et al., 2020). These basins include the mid-Cretaceous to Eocene Black Sea basin, which still exists today, and the Jurassic-Cretaceous Greater Caucasus basin, which was consumed by a small subduction zone forming the Caucasus fold-thrust belt since the late Eocene (Cowgill et al., 2016; Cavazza et al., 2024). Caucasus shortening accounts for ~30% of the Arabia-Eurasia convergence since the Oligocene, i.e., ~250 km (Cowgill et al., 2016). This shortening gradually decreased west- and eastward, causing northward convex oroclinal bending that also affected the eastern Anatolian orogen to its south (van der Boon et al., 2018). South of the Lesser Caucasus Block, a small continental fragment, the South Armenian Block collided with the Lesser Caucasus in the Late Cretaceous. After this collision, subduction transferred to its south, within northeastern Anatolia (Nikogosian et al., 2023; Sosson et al., 2010; van Hinsbergen et al., 2020).

The Pontides and the South Armenian Block are bounded to the south by the Izmir-Ankara-Erzincan Suture zone and the Kağızman-Khoy Suture, respectively, separating them from the eastern Tauride nappes (Figure 2). The Tauride fold-thrust belt underlies most of eastern Anatolia and also includes the Bitlis Mountains. In eastern Anatolia, the rocks of the Tauride fold-thrust belt are almost everywhere metamorphosed showing they have been deeply buried and were subsequently exhumed (Kuşcu et al., 2010; Oberhänsli et al., 2014; Topuz et al., 2017). The eastern Tauride fold-thrust belt is separated from the Arabian continent by the Bitlis Suture (Figure 2).

The Taurides contain thrusted remains of the continental crust of the 'Greater Adria' microcontinental realm, which extended westwards to the circum-Adriatic region of the Central Mediterranean (van Hinsbergen et al., 2020). This continental lithosphere was separated from Eurasia and Africa-Arabia by northern and southern Neotethyan oceanic branches, respectively, within which intra-oceanic subduction occurred in the Late Cretaceous (~100-90 Ma), and remains of which are found as ophiolites. These ophiolites and underlying mélanges now form the highest structural units of the Tauride fold-thrust belt and were also thrust southwards onto the Arabian continental margin (Yılmaz et al., 1993; Robertson et al., 2007; see detailed review and reconstruction in Maffione et al., 2017; van Hinsbergen et al., 2020) (Figures 3 and 4). Below these ophiolites, continental lithosphere of Adria was subducted. The upper crust of this subducted lithosphere accreted as nappes, starting within 10 Ma after subduction initiation (Topuz et al., 2017). Accretion and nappe stacking of Greater Adria continental crust continued into the Eocene in central and western Anatolia (McPhee et al., 2018) but in the easternmost Anatolia, Greater Adria was narrower and its subduction and accretion of its upper crust - becoming the easternmost Taurides, likely occurred entirely within the Late Cretaceous (Yilmaz, 1994; Topuz et al., 2017; Kuşcu et al., 2010; 2013).

The Cretaceous nappe stacking episode in the east Anatolian portion of Greater Adria was particularly complex because the eastern Mediterranean ocean, separated Greater Adria from Arabia/Africa, became invaded by an east-dipping subduction zone that rolled back westward, passing between eastern Greater Adria and Arabia between ~90 and 80 Ma (Moix et al., 2008; van Hinsbergen et al., 2020). This process led to ophiolite obduction both to the north, onto southern Greater Adria, and to the south, onto northern Arabia (Figures 3 and 4). Eastern Greater Adria thus became obducted from north, east, and south.

In the Paleogene, after the subduction and accretion of Greater Adriatic continental crust to the upper oceanic lithosphere of the Neotethys, northward subduction of oceanic lithosphere that separated Greater Adria from Arabia occurred - which since the preceding roll-back invasion consisted of Cretaceous back-arc basin lithosphere (Figures 3 and 4). During this time, the Tauride accretionary fold-thrust belt was intruded by a widely distributed magmatic arc (Kuşcu et al., 2010; 2013). In Paleocene to Oligocene time, this eastern Tauride nappe stack must have undergone large-scale, regional extension: deep, crystalline portions of the orogen and arc were exhumed and yielded apatite fission track ages ranging from 35-55 Ma in the interior part of the east Anatolian plateau (Albino et al., 2014). Unconformably overlying terrestrial, volcanic, and marine sediments are also lower to upper Paleogene in age (Yilmaz et al., 2010; Kuşcu et al., 2013). In the south of the orogen, in the forearc above the Bitlis subduction zone, the deep-marine, extensional Maden and Hakkari forearc basins formed (Aktaş and Robertson, 1984; Robertson et al., 2007). Extension continued into the Oligocene, e.g., in the Muş Basin (Hüsing et al., 2009). These basins show that extension ceased and shortening and thrusting started in the late Oligocene (Aktaş and Robertson, 1984; Hüsing et al., 2009) and continued throughout the Miocene (Koçyiğit et al., 2001; Yusufoğlu, 2013). This onset of shortening predated the arrival of the northern Arabian margin at the Bitlis subduction zone in early to middle Miocene time. The latter is dated from focused uplift and exhumation dated by ~18 Ma fission track data in the Bitlis Massif (Cavazza et al., 2018: Okay et al., 2010, Figure 3; see next section).

Simultaneously with the closure of the southern Neotethys Ocean, the northern branch between the Taurides orogen and the Pontides also closed (Figures 3 and 4). The closure of this northern branch was diachronous, becoming younger eastwards across Anatolia (Gürer and van Hinsbergen, 2019). In western and central Anatolia, this closure occurred from latest Cretaceous to Paleocene time (Mueller et al., 2019; Ocakoğlu et al., 2019), and Africa-Eurasia convergence was accommodated by oceanic subduction at the Cyprus trench until the first continental crust of the North African margin arrived in the late Miocene (~9 Ma) (McPhee and van Hinsbergen, 2019). In eastern Anatolia, however, subduction must have continued later, since hundreds of kilometers of convergence between the Taurides and Pontides must have occurred after the early Eocene (Gürer and van Hinsbergen, 2019).

This amount of convergence is estimated from a paleomagnetically documented regional counterclockwise rotation of ~30° of the eastern southern and eastern Tauride Orogen relative to the Pontides since the latest Oligocene-early Miocene (~25-20 Ma) (Cinku, 2017; Cinku et al., 2017; Gürer and van Hinsbergen, 2019; Gürer et al., 2018). Convergence and shortening between the eastern Taurides and the eastern Pontides must have continued until the arrest of rotation, which remains poorly understood. The youngest documented shortening in the Sivas Basin is Late Miocene in age (Poisson et al., 2015; Kergaravat et al., 2017). Demonstrated shortening magnitudes in the Sivas basin are on the order of only kilometers (Legeay et al., 2019; Darin and Umhoefer, 2019), significantly less than contemporaneous regional convergence required to accommodate vertical axis rotations. The Sivas thrust or the Deliler-Tecer fault, which bound and dissect the Sivas Basin, respectively, may thus have accommodated much more shortening than the reconstructed minimum values (Darin and Umhoefer, 2019, Gürer and van Hinsbergen, 2019).

In summary, the eastern Anatolian orogenic crust experienced distributed, intense, and polyphase deformation in response to accretion and the closure/termination of multiple subduction systems (Figures 3 and 4). When these subduction zones ceased, and whether this process was diachronous remains poorly constrained. Within this complex, multiphase deformed orogenic collage, the North and East Anatolian Faults started forming in Late Miocene time, eventually delineating the Anatolian microplate.

3. Neogene deformation in eastern Anatolia

To reconstruct how the extruding Anatolian microplate developed in the East Anatolian Plateau, we first review the available, but sparse, constraints on Neogene fault displacements in eastern Anatolia. Next, we reconstruct these faults in the context of regional plate motion. The amount and rate of Africa-Arabia-Eurasia convergence are determined from reconstructions of a plate circuit. Relative Arabia-Eurasia plate motion is reconstructed in detail based on marine magnetic anomalies in the North Atlantic Ocean between Eurasia and North America and in Central Atlantic Ocean between North America and Africa and for the Red Sea basin between Africa and Arabia, with approximately one anomaly per million years (DeMets et al., 2015; DeMets and Merkouriev, 2016). For the reconstruction of the Caucasus orocline, we adopt the reconstruction of van der Boon et al. (2018). This restoration is based on paleomagnetic constraints that predict since the late Eocene, up to 300 km of Arabia-Eurasia convergence was accommodated in the Caucasus region, to the north of the South Armenian Block. This convergence is consistent with and includes shortening estimates based on seismological and structural geological observations (e.g., Alania et al., 2015; Trexler et al., 2020; Gusmeo et al., 2021). For the long-term evolution of Anatolia since the Mesozoic, we use the reconstruction of Mediterranean orogenic belts by van Hinsbergen et al. (2020).

The present-day Anatolian microplate is separated from the Eurasian Plate by the dextral North Anatolian Fault Zone, extending to the Karlıova 'triple junction' (Şengör, 1979). Here, it merges with the Varto Fault Zone, a thrust system, and the East Anatolian Fault Zone (Karaoğlu et al., 2017; Sançar et al., 2015) (Figures 3 and 5). The East Anatolian Fault Zone ends to the southwest in the Amik (or Hatay) Triple Junction, where it meets the Cyprus Trench that separates Anatolia and Africa, and the Dead Sea transform fault that separates Africa from Arabia (Duman and Emre, 2013; Tarı et al., 2013) (Figures 3 and 5). However, the Anatolian micro-'plate' and the southern Eurasian margin are not rigid, but they experienced regional deformation. Active fault zones within the Anatolian microplate include those that branch southward off the North Anatolian Fault and the Malatya-Ovacık Fault (Figure 2). Even though they are active, these faults are at present subordinate to the North and East Anatolian Fault zone displacements (Emre et al., 2018; Higgins et al., 2015; Koçyiğit and Beyhan, 1998). Additionally, the westward decreasing Caucasus shortening also affects the southern

Eurasian margin to the north of the eastern part of the North Anatolian Fault, causing an overall sinistral shear between areas south, and west of the longitude of the Caucasus (Simão et al., 2016; Emre et al., 2018).

The onset of formation of the 1400 km long North Anatolian Fault Zone is estimated from terrestrial stratigraphy in transtensional basins to have occurred around ~13-11 Ma (Şengör et al., 2005). U/Pb dating of tectonic calcite fabrics from the North Anatolian Fault zone in central and western Anatolia yielded an age of 11 Ma age (Nuriel et al., 2019). However, whether the North Anatolian Fault Zone formed simultaneously along its entire modern length is uncertain: evidence from basins and offset markers in the western portion of the fault zone has been used to argue for a westward propagation of the fault zone, reaching the Aegean domain only in Pliocene time (Racano et al., 2023; Sakellariou and Tsampouraki-Kraounaki, 2019; Şengör et al., 2005). The total offset of the North Anatolian Fault Zone has been estimated at up to 85 km (Akbayram et al., 2016; Hubert-Ferrari et al., 2002; Şengör et al., 2005), although reconstructions of the Aegean region account for only some tens of kilometers of motion (van Hinsbergen et al., 2006). It is possible that some tens of kilometers of displacement (Hubert-Ferrari et al., 2009) may thus have been accommodated within central or western Anatolia, although the specifics of where and how remain unclear (van Hinsbergen et al., 2020). In our discussions, we use the maximum-displacement estimate of 85 km right-lateral slip along the North Anatolian Fault Zone since 13 Ma.

The Karlıova Triple Junction at the eastern termination of the North Anatolian Fault is a transform-transform-thrust triple junction that migrates WNW-ward along the North Anatolian Fault. To the east of the Karlıova Triple Junction, the Varto Fault Zone exhibits a similar orientation as the North Anatolian Fault (Figures 3 and 5). Currently, it is a seismically active thrust zone that accommodates part of the Arabia-Eurasia convergence (Sançar et al., 2015). Horizontal striations on fault surfaces indicate its past role as a strike-slip fault zone when the triple junction was positioned farther east (Karaoğlu et al., 2017). The exposed length of the fault zone is 35 km providing a minimum westward migration of the Karlıova Triple Junction since the formation of the East Anatolian Fault Zone, but its eastward continuation may be buried below young volcanics (Figure 3): if not, the 35 km length of the Varto Fault Zone represents the maximum displacement since the formation of the East Anatolian Fault Zone. There is no estimate for the N-S shortening accommodated by the Varto Fault

Zone, but it likely accommodated only a small portion of the late Neogene Arabia-Eurasia convergence. This is demonstrated by the numerous active E-W trending thrust faults and strike-slip faults mapped between the Bitlis suture zone in the south and the Caucasus in the north (Emre et al., 2018; Koçyiğit et al., 2001), including those that ruptured during the 2011 Mw 7.1 Van earthquake (Elliott et al., 2013). However, these faults are laterally discontinuous at the surface, suggesting they are mostly blind, and/or buried below young volcanic deposits. They are widely distributed, and their cumulative displacement since the Miocene has not been previously estimated.

The onset of the East Anatolian Fault Zone is estimated to be much younger than that of the North Anatolian Fault Zone: only 6-3 Ma. These estimates are indirect at best: they are based on an assumed link between 6 Ma volcanism and deformation in the Karlıova Triple Junction region (Karaoğlu et al., 2017), the interpretation that 5 Ma thermal resetting of fission track ages along the fault zone results from fluids and assuming that these fluids mark the onset of the East Anatolian Fault (Whitney et al., 2023), and the ages of displaced volcanic and sedimentary rocks (Westaway and Arger, 2001). The most direct/robust age indication comes from the Elbistan Basin, located just north of the Sürgü Fault (Yusufoğlu, 2013). This basin is an early Pliocene terrestrial pull-apart basin that formed between left-lateral strike-slip faults, within folded lower to upper Miocene marine sediments. These observations indicate a regional change from compressional deformation to strike-slip-dominated deformation around the beginning of the Pliocene, i.e. ~5 Ma (Yusufoğlu, 2013). This is consistent with observations across the east Anatolian plateau around the North and East Anatolian Faults, where Miocene strata are folded, but upper Pliocene and younger volcanic rocks that are widespread in the region, are not (Koçyiğit et al., 2001). Offset markers showed between ~15 and 27 km of total displacement of the East Anatolian Fault Zone (Şaroğlu, 1992; Yönlü et al., 2013). The E-W oriented Sürgü Fault, along which the M_w 7.7 2023 Ekinözü earthquake occurred (Liu et al., 2023) (Figures 3 and 5), functions as a left lateral strike-slip fault with reverse component (Balkaya et al., 2021; Duman et al., 2020; Koç and Kaymakcı, 2013). This fault connects westward to the Yakapınar-Göksun Fault that transfers its slip towards the Cyprus trench (Koç and Kaymakcı, 2013; Westaway, 2004). In recent times, the Sürgü Fault is taking up approximately one third of the total plate boundary slip, but prior to the Pliocene, it acted as thrust fault with a dextral component that accommodated part of the Arabia-Eurasia convergence (Koç and Kaymakcı, 2013).

If the East Anatolian Fault did not exist until ~6-5 Ma, but the North Anatolian Fault did, then the Arabia-Anatolia (micro)plate boundary must have been located farther west before this time (Kaymakcı et al., 2010; Westaway and Arger, 2001). Candidate fault zones representing this former (micro)plate boundary are NE-SW trending faults inferred from mapped, abrupt discontinuities in the Taurides fold-thrust belt (Kaymakcı et al., 2010), such as the Göksün and Malatya-Ovacık Faults (Figure 2). Of these, only the Malatya-Ovacık Fault has been studied in detail in the field. This fault is seismically active, accommodating 2-3 mm/a of left-lateral motion (Sançar et al., 2019; 2020). Field studies have shown that between 5 and 3 Ma, it accommodated a left-lateral displacement of ~29 km (Westaway and Arger, 2001). The Malatya-Ovacık Basin had already formed by transtension in early to mid-Miocene time (Kaymakcı et al., 2010), but there is no estimate of pre-Pliocene fault displacements. A minimum of 20 km of displacement of the NNE-SSW trending Göksün Fault (not to be confused with the Yakapınar-Göksun Fault, Figure 3) that cuts through the eastern Taurides was estimated based on the horizontal offset of mapped units (van Hinsbergen et al., 2020). However, no detailed field study has been performed to corroborate apparent horizontal displacement. Farther west, the Ecemiş Fault (Figure 2) is a prominent structure that transferred Arabia/Africa-Eurasia convergence to the Sivas Basin region and culminated in a late Eocene to early Miocene displacement of the Tauride fold-thrust belt of 60-80 km (Gürer et al., 2016; Jaffey and Robertson, 2001). However, the Ecemiş Fault is sealed in the south by lower Miocene sediments, and younger motion only involved minor transtension with an E-W extensional component (Gürer et al., 2016; Higgins et al., 2015, Jaffey and Robertson, 2001): it therefore did not play a significant role in the development of the Anatolian microplate.

During the Miocene, the Bitlis Massif was thrust over the Arabian continental margin, as well as onto the ophiolites that were obducted onto that margin in the Late Cretaceous (Oberhänsli et al., 2010). These overthrust ophiolites are exposed in a window 40 km north of the Bitlis thrust front, providing a minimum amount for the Miocene thrust displacement (Oberhänsli et al., 2010; Yılmaz et al., 1981). Low-temperature thermochronology revealed cooling ages of the Bitlis Massif between ~18 and 13 Ma, which is interpreted as the result of underthrusting of the Arabian continental margin below the Bitlis (Cavazza et al., 2018; Okay et al., 2010). The Muş Basin that overlies the Bitlis massif to the north was uplifted in the middle Miocene (Huvaz, 2009), and sedimentary successions overlying the northeastern margin of the Bitlis Massif were uplifted from deep-marine to terrestrial conditions between 19 and 17 Ma (Gülyüz et al., 2020). This suggests that the Arabian continental margin first began to underthrust the Bitlis Massif around 19-18 Ma and continued to do so until at least ~13 Ma. Finally, between 13 and 11 Ma, a 6 km thick pile of deep-marine turbidites in the Kahramanmaraş Basin, located on the northwestern margin of Arabia (Figure 2) that was overthrust by the eastern Tauride orogen (Hüsing et al., 2009). This indicates that the thrusting of the eastern Tauride orogen over the Arabian margin became progressively younger to the west. There is currently no geological evidence suggesting significant Arabian underthrusting below the Bitlis Massif after 11 Ma. At present, the faults between the Bitlis Massif and Arabia display limited seismicity (Tan et al., 2008) (Figure 5).

4. Reconstruction

We now use the plate circuit and the known fault displacements and ages summarized above to evaluate how much Arabia-Eurasia convergence was accommodated by westward block extrusion away from the collision zone, and where else Arabia-Eurasia convergence may have been accommodated within the east Anatolian orogen. The plate circuit reveals that Arabia-Eurasia convergence has been ~2 cm/a throughout the Neogene. The youngest known age for the activity of the Bitlis Suture Zone of ~11 Ma (Cavazza et al., 2018; Faccenna et al., 2006; Hüsing et al., 2009; Okay et al., 2010; Şengör et al., 2003) coincides with the estimates for the onset of North Anatolian Fault activity at 13-11 Ma (Nuriel et al., 2019; Şengör et al., 2005) and an estimate for the timing of slab break-off at the Bitlis suture zone of 13-11 Ma age, which is based on a magmatic flare-up (Keskin, 2003). We therefore first evaluate whether this time could coincide with an abrupt change from subduction to extrusion, such that Anatolian extrusion may have accommodated all post-11-13 Ma Arabia-Eurasia convergence. To this end, we simplify the geometry of Anatolia to a schematic representation of the North and East Anatolian Faults and temporarily disregard the complexity that the Arabia-Anatolia plate boundary prior to ~5-6 Ma was likely located or distributed along faults farther west (Figure 6). We will incorporate this complexity to our analysis later.

The Eurasia-North America-Africa-Arabia plate circuit, constrained by magnetic anomalies in the Atlantic Ocean and Red Sea (DeMets et al., 2015; DeMets and Merkouriev, 2016), shows that since the onset of the North Anatolian Fault formation at 13 Ma, ~270 km of NNW-SSE convergence was accommodated at a location coinciding with the Karlıova Triple Junction (Figure 6). To accommodate all this convergence through extrusion, the wedge-shaped microplate defined by the North and East Anatolian faults would have to be restored as much as 375 km eastwards along the North Anatolian Fault at 13 Ma. Such a displacement is far greater than the maximum field-based estimate of 85 km (Akbayram et al., 2016; Hubert-Ferrari et al., 2002; Şengör et al., 2005). Restoring this maximum displacement estimate for the North Anatolian Fault instead reveals that no more than ~65 km of NNW-SSE Arabia-Eurasia convergence could have been accommodated by westward extrusion since 13 Ma (Figure 6; Supplementary movie). This means that since the onset of formation of the North Anatolian Fault, >200 km of Arabia-Eurasia convergence must have been accommodated by shortening elsewhere in the eastern Anatolian orogen, to the south and/or north of the North and East Anatolian Faults. Moreover, to the east of the Karlıova Triple Junction, all convergence must have been accommodated by shortening within the orogen. That region lies to the south of the Caucasus region, where approximately a third of this convergence may have been accommodated (Forte et al., 2022; van der Boon et al., 2018). The remainder must have been accommodated within the east Anatolian orogen.

5. Discussion

5.1 How was Arabia-Eurasia convergence partitioned in eastern Anatolia?

Our reconstruction shows that Anatolian extrusion since the formation of the North Anatolian Fault Zone around 13-11 Ma cannot account by itself for the entire amount of contemporaneous Arabia-Eurasia convergence in eastern Anatolia (Figure 6). From this, we infer that throughout much of its extrusion history, the eastern Anatolian orogen must have accommodated shortening of ~200 km and the extrusion-accommodating transform faults must have developed within a deforming orogenic belt

(Figure 6; Supplementary movie). Because at the present-day, extrusion is more or less balancing Arabia-Eurasia convergence west of the Karlıova Triple Junction (Reilinger et al., 2006), extrusion must have accelerated through time. This is consistent with evidence that the onset of slip on the North Anatolian Fault becomes younger along the fault zone, only reaching the strands in western Anatolia in the Pliocene (Hubert-Ferrari et al., 2009; Racano et al., 2023; Şengör et al., 2005, Sakellariou and Tsampouraki-Kraounaki, 2019). Consequently, pre-Pliocene strike-slip displacements must have been accommodated within central Anatolia, but where and how is poorly known. Major structures such as the Ecemiş Fault, and the enigmatic Central Anatolian Fault zone (or Deliler-Tecer Fault Zone) that runs through the Sivas Basin, have little post-early Miocene displacement (Gürer et al., 2016; Jaffey and Robertson, 2001; Koçyiğit and Beyhan, 1998; Higgins et al., 2015, Darin and Umhoefer, 2019). The absence of compressional belts within Central Anatolia, which could form splays accommodating North Anatolian Fault displacement, suggests that its pre-Pliocene motion was indeed limited. Particularly for the late Miocene, but also in the Plio-Pleistocene, Arabia-Eurasia convergence in eastern Anatolia must therefore mostly have been accommodated by N-S shortening. This marks a 'transition period' (Koçyiğit et al., 2001) between the onset of extrusion-accommodating strike-slip fault formation and the establishment of the present-day Anatolian 'microplate'.

Finding how (discrete vs. distributed) and where this late Miocene and younger shortening component of ~200 km - and even more lower to middle Miocene convergence that followed upon the arrival of the Arabian continent at the Bitlis margin - was accommodated is not straightforward. To illustrate, this amount of shortening is of a similar magnitude as was reconstructed for the Pyrenees (Muñoz, 1992) or the southern Andes (Schepers et al., 2017). In the youngest major mapped thrust zones that could have localized such convergence, such as in the Sivas Basin or the Bitlis Suture Zone, only kilometer-scale late Miocene and younger shortening has been recognized so far (Hüsing et al., 2009; Legeay et al., 2019, Darin and Umhoefer 2019). However, paleomagnetic data have demonstrated regional rotation differences indicating large-scale orogenic deformation since the middle Miocene (Cinku, 2017; Cinku et al., 2017; Gürer and van Hinsbergen, 2019; Gürer et al., 2018). The paleomagnetic rotations of the pre-Neogene Tauride Orogen may be used as a marker to assess how the 'missing' convergence was distributed roughly north and south of the central axis of the fold-thrust belt. Reconstructing the paleomagnetic evidence from the eastern Tauride Orogen from central to eastern Anatolia for a coherent, ~30° counterclockwise vertical axis rotation since the late Oligocene-early Miocene, ~25-20 Ma (Cinku, 2017; Cinku et al., 2017; Gürer et al., 2018) around a rotation pole marked by an orocline recognized in central Anatolia (Gürer and van Hinsbergen, 2019; Lefebvre et al., 2013) allows to keep the Bitlis massif attached to the north Arabian margin in the late early to middle Miocene (Figure 7, Supplementary Movie). This is consistent with the estimated collision age from geological reconstructions (Cavazza et al., 2018; Okay et al., 2010), while at the same time maintaining the connection of the eastern Taurides to Central Anatolia (Gürer and van Hinsbergen, 2019; van Hinsbergen et al., 2020) (Figure 7). This rotation also explains why the onset of thrusting of the eastern Tauride orogen over the Arabian continental margin was diachronous, becoming younger westwards, consistent with the observations from Kahramanmaraş, where foreland basin sedimentation and Arabian underthrusting continued until 11 Ma (Hüsing et al. 2009). Restoring the full 30° counterclockwise block rotation since the Oligocene however, requires that shortening between the eastern Taurides and eastern Pontides started before the collision of Arabia with the eastern Taurides (Bitlis) massif, consistent with evidence for Oligocene shortening in the Sivas Basin (Legeay et al., 2019). This rotational deformation of the eastern Taurides suggests that post-early Miocene shortening to the north of the Tauride Orogen (i.e., in the Sivas Basin region and along-strike towards the east (Gürer et al., 2018)) increases eastwards. Meanwhile, the amount of post-early Miocene convergence accommodated by the Cyprus trench and Bitlis Suture Zone decreases eastwards. In other words, almost all post-collisional Arabia-Eurasia convergence (up to 450 km since 20 Ma) was accommodated north of the Bitlis suture zone and south of the Central Anatolian Taurides (Figures 4 and 7).

We may further constrain the distribution of shortening by estimating displacements of the strike-slip faults that cut through the Tauride Orogen. For instance, the left-lateral displacement of the Malatya-Ovacık fault zone between 5 and 3 Ma transferred an estimated 28 km of convergence from the south to the north of the Tauride Orogen (Westaway and Arger, 2001). Determining the timing and amount of displacement of the other strike-slip faults and associated basins cutting through the eastern Taurides, mapped by Kaymakcı et al. (2010), such as the Göksün Fault (Figure

3), may thus identify further where the shortening was partitioned over the Sivas basin and its eastern continuation or the Bitlis Suture Zone.

5.2 Uplift mechanisms of the Anatolian Plateau

The recognition that extrusion was likely an accelerating process, gradually taking an increasing component of the convergence may shed light on potential triggers for extrusion. Often-quoted causes point at tectonic stresses caused by Arabia-Eurasia convergence, combined with a westward gradient caused by excess gravitational potential energy and perhaps associated mantle flow, due to East Anatolian Plateau rise in the east combined with Aegean extension and subsidence in the west (Faccenna et al., 2006; Le Pichon and Kreemer, 2010; Sternai et al., 2014; Whitney et al., 2023). Aegean extension started well before extrusion, around 45 Ma, and accelerated around 25 and 15 Ma (Brun and Sokoutis, 2010; Philippon et al., 2014; van Hinsbergen and Schmid, 2012). Hence, while this extension may have preconditioned westward extrusion, its onset or evolution does not provide an obvious trigger for the extrusion. The rise of the East Anatolian Plateau, however, coincides more closely with the onset of extrusion: when the North Anatolian Fault started to form in the middle Miocene, marine sedimentation still occurred in regions now uplifted by a kilometer or more (Gülyüz et al., 2020; Legeay et al., 2019; Şengör et al., 2008; Yusufoğlu, 2013). Plateau rise in general may have several causes, including crustal shortening and thickening, continental underthrusting, or dynamic and isostatic topographic rise due to slab break-off or various forms of mantle lithospheric delamination (Göğüş and Pysklywec, 2008; Keskin, 2003; Memiş et al., 2020; Şengör et al., 2003; Uluocak et al. 2021). These processes may all contribute at different times and locations, as they likely did in Central Anatolia (McPhee et al., 2022). For eastern Anatolia, dynamic topographic rise is so far the favored interpretation (Faccenna et al., 2006; Keskin, 2003; Memiş et al., 2020; Molin et al., 2023; Şengör et al., 2003; Whitney et al., 2023). For instance, seismic tomographic evidence shows a broken-off 'Bitlis' slab in the upper mantle below the northern Arabian margin in eastern Anatolia (Faccenna et al., 2006; Hafkenscheid et al., 2006). A middle Miocene volcanic flare-up in the East Anatolian Plateau may date that event at 13-11 Ma (Keskin, 2003) and slab break-off may thus have contributed to early topographic rise. However, slab break-off effects are typically limited to the region directly above the breaking slab, not the entire upper plate plateau (Buiter et al., 2002; Göğüş and Pysklywec, 2008; Memiş et al 2020).

Another possible cause for uplift is the underthrusting of buoyant continental crust (e.g., Kapp and Guynn, 2004; van Hinsbergen, 2022). Following Bitlis slab break-off, horizontal underthrusting of Arabian lithosphere occurred; seismological observations suggest that it currently protrudes 100 ± 50 km below eastern Anatolia (Whitney et al., 2023). Whitney et al. (2023) postulated that horizontal Arabian underthrusting below the orogen started 5 Ma ago and triggered the formation of the East Anatolian Fault and thereby established a rigid Anatolian microplate. However, this hypothesis would require that all post-5 Ma Arabia-Eurasia convergence was accommodated by Arabian underthrusting below the Bitlis massif, whereas there is no evidence that significant thrusting south of the Bitlis massif occurred after 11 Ma. Moreover, geological reconstructions and GPS vectors reveal that ~30% of Pliocene Arabia-Eurasia convergence was accommodated in the Caucasus (Cowgill et al., 2016; van der Boon et al., 2018). Therefore, the horizontal underthrusting of Arabia below the eastern Tauride orogen must thus be older and likely occurred in the period directly preceding slab break-off. While thus underthrusting contributed to uplifting the southern part of the East Anatolian Plateau, as shown by the reset low-temperature thermochronometers (Cavazza et al., 2018), it is not a likely trigger for East Anatolian Fault formation and is unlikely to be the sole trigger for extrusion.

The seismological observations showing a 45 km thick crust but only a thin mantle lithosphere (Barazangi et al., 2006) have led to arguments that lithosphere removal could have caused rapid topographic rise since the middle Miocene (Şengör et al., 2003). Mechanisms for delamination of a hypothetical mantle lithosphere below the East Anatolian plateau were later explored through numerical modeling and shown to be physically plausible, under the assumption that eastern Anatolia already had a thick crust in the middle Miocene, and was underlain by a thick mantle lithosphere to delaminate (Göğüş and Pysklywec, 2008; Memiş et al., 2020). However, in the light of the longer orogenic history, the availability of a thick mantle lithosphere to delaminate in the Miocene is questionable (Figure 4). The continental subduction that formed Tauride accretionary orogen consisting of only upper crustal continent-derived nappes in the Late Cretaceous, the original Greater Adriatic lithosphere that underpinned these nappes, subducted. Such a process leaves a thick crust, but no mantle lithosphere

(Jolivet and Brun, 2010; van Hinsbergen et al., 2005; van Hinsbergen and Schouten, 2021). The absence of a thick mantle lithosphere below the East Anatolian Plateau that is taken as key argument for Miocene delamination (e.g. Memiş et al., 2020), is not unique to the East Anatolian Plateau: neither the Anatolian nor the Aegean accretionary orogen is associated with a thick lithosphere. Instead, they have a thin lithosphere that re-grew by cooling after nappe stacking (e.g., Endrun et al., 2011).

Geological evidence shows that after the stacking of the nappes, the orogen was extended throughout the Paleogene, forming basins such as the Maden and Mut Basins (Aktaş and Robertson, 1984; Hüsing et al., 2009; Robertson et al., 2007). This extension lead to the widespread exhumation of metamorphic and igneous rocks found on the east Anatolian Plateau (Kuşcu et al., 2010). This extension and exhumation must have been associated with thinning of the nappe stack, which explains the widespread unconformable marine sedimentary cover of late Eocene to Miocene age (Figure 7). Consequently, the modern orogenic architecture of the east Anatolian Plateau suggests a tectonic history in which the crust in the Miocene was thin, and not associated with a thick mantle lithosphere. In fact, the east Anatolian region was tectonically and paleogeographically similar to the modern Aegean region: a crust consisting of accreted nappes, stretched and thinned and associated with widespread exhumation of metamorphic and igneous rocks, largely submarine, and underlain by a thin lithosphere (e.g., van Hinsbergen et al., 2005; Jolivet and Brun, 2010; Endrun et al., 2011; Schmid et al., 2020). These conditions are quite different from those used in numerical models to evaluate plateau rise by delamination of a lithospheric root (e.g., Memiş et al., 2020).

Instead, we infer that crustal thickening and shortening must have played a central role in developing the high East Anatolian Plateau. The post-13 Ma shortening component of ~200 km, as determined from the Arabia-Eurasia plate circuit, is similar to the width of the East Anatolian Plateau around Karlıova, and is thus enough to have shortened the crust by ~50% since the onset of formation of the North Anatolian Fault, and even more since the arrival of the Arabian continental margin at the Bitlis margin (Figures 3, 4 and 7). Such shortening may straightforwardly explain the modern crustal thickness and the uplift of the Miocene sedimentary cover (Gülyüz et al., 2020; Legeay et al., 2019; Şengör et al., 2008; Yusufoğlu, 2013). It is of course possible that a thin lithosphere, thermally regrown after Cretaceous nappe stacking, was sufficiently thickened during this shortening process and subsequently delaminated again, as argued for central Anatolia (Göğüş et al., 2017). This delamination would then have further enhanced uplift, but we infer that regionally distributed, large-scale crustal thickening was the main driver of Neogene East Anatolian plateau rise.

Geological evidence also shows that the onset of this shortening predates the onset of extrusion, both in the Sivas Basin and its eastern continuation (Legeay et al., 2019) and in the Bitlis Massif (Cavazza et al., 2018). It may even predate the arrival of the Arabian margin in the trench below the Tauride orogen (Figure 3). For both eastern Anatolia and the Caucasus (Cowgill et al., 2016; Vincent et al., 2007), the onset of upper plate shortening may well relate to the dynamics of the subduction zones involved and similarly to many other orogens (e.g. the Andes, pre-Cenozoic Tibet), the onset of upper plate shortening is not correlated with the onset of continental 'collision', i.e. the first arrival of a continental margin in a subduction zone (van Hinsbergen and Schouten, 2021). From the available evidence, we do not see a direct causal relationship in space and time between the arrival of the Arabian continent in the trench ('collision') and the onset of extrusion and microplate formation. Rather, Anatolian extrusion and the formation of the modern microplate developed gradually in a regionally shortening orogen. Extrusion may have been facilitated by a low topography in the west due to Aegean extension, the availability of weakness zones along which strike-slip fault zones could localize in Anatolia, and the progressive increase of gravitational potential energy in the east due to crustal thickening-driven uplift. Over time, these processes accelerated in a progressively rotating, shortening, and thickening orogenic belt that originated in the upper plate of a complex, long-lived subduction system. The regional counterclockwise rotation of the eastern Tauride Orogen gradually changed the orientation of its pre-existing weakness zones through time, which may have underpinned the activation and abandonment of fault segments throughout the transition period. This eventually led to the eastward stepping of the Anatolian 'plate boundary' to the East Anatolian Fault in the Pliocene.

Finally, it is disconcerting that as much as 400 km of 'post-collisional' convergence, of which ~200 km post-'microplate' formation, appears challenging to identify in the geological record. Identifying how and where this shortening was and is being accommodated requires new, detailed field studies of the structures cutting and flanking the East Anatolian Plateau. The lack of a connected mosaic of surface traces of the thrust faults across the plateau suggests that many of them are blind or buried below the widespread Plio-Quaternary volcanic cover, calling for detailed and integrated geomorphological, geophysical, and geological field studies. The structures accommodating this convergence, even if blind, may still be active and pose considerable seismic risk, as illustrated by the devastating, thrust-related October 23, 2011 M_w 7.1 Van earthquake (Fielding et al., 2013). A detailed, integrated study of the structure and tectonic history of the East Anatolian Plateau, from the early stacking of nappes, through the subsequent regional extension and exhumation, and including the Neogene shortening during the uplift of the plateau and the onset of extrusion, will offer key insights into the dynamics and hazards of the East Anatolian Plateau.

Conclusions

Our kinematic reconstruction of the Neogene evolution of the Eastern Anatolian Orogen shows that, even with the maximum estimates for displacement of Anatolia along the North Anatolian Fault, Anatolian extrusion cannot account for more than 65 km (i.e. ~25%) of the total of ~275 km of Arabia-Eurasia convergence since the onset of extrusion 13 Ma ago. In the absence of wholesale subduction, the remainder of this convergence must have been accommodated by crustal shortening and thickening. We use a kinematic reconstruction cast in the Arabia-Eurasia plate circuit to identify where this shortening may have been accommodated, but we stress that detailed, integrated geological, geophysical, and geomorphological field studies are required to identify where and in what fashion this convergence was geologically accommodated. We show that the East Anatolian Plateau is underlain by an orogen that underwent nappe stacking below ophiolites in the Late Cretaceous, which must have developed a thick crust but without the originally underlying mantle lithosphere that was lost to subduction. This nappe stack subsequently extended leading to widespread crystalline rock exhumation and marine sedimentation, followed by Neogene regional shortening that must have accommodated a few hundred kilometers of convergence. We postulate that orogenic shortening was likely the main driver of East Anatolian Plateau rise. Because the orogen underlying the plateau already lost its lithospheric underpinnings during Cretaceous orogenesis, we consider delamination and dynamic topographic rise a less likely contributor to plateau rise. Finally, we stress that detailed field studies are urgent in identifying the young orogenic history, and that structures accommodating orogenic shortening may still pose seismic hazards, besides the well-known hazards of Anatolia’s prominent strike-slip system.

Acknowledgements

DJJvH acknowledges NWO VICI grant 865.17.001. William Cavazza and Oğuz Göğüş are warmly thanked for their critical and constructive reviews.

Figure captions

Figure 1: Anatolian Microplate and main tectonic elements within the framework of the major plates around the eastern Mediterranean region. AT = Aegean Trench; CT = Cyprus Trench; EAFZ = East Anatolian Fault Zone; NAFZ = North Anatolian Fault. Inset shows location of Fig. 2.

Figure 2: Detailed geological map, modified after the Geological Map of Turkey (Şenel, 2002). Abbreviations: AB = Adana Basin; ATJ = Amik Triple Junction; BM = Bitlis Massif; BS = Bitlis Suture; CAFZ = Central Anatolian Fault Zone; EAFZ = East Anatolian Fault Zone; EF = Ecemiş Fault; HB = Hakkari Basin; IAS = İzmir-Ankara Suture; NAFZ = North Anatolian Fault Zone; PM = Pötürge Massif; SB = Sivas Basin; SF = Sürgü Fault; KKS = Kağızman-Khoy Suture; KTJ = Karlıova Triple Junction; LV = Lake Van; MB = Maden Basin; MOF = Malatya-Ovacık Fault; MuB = Muş Basin; GF = Göksün Fault; KB = Kahramanmaraş Basin; VFZ = Varto Fault Zone; YGF = Yeşilgöz-Göksün Fault.

Figure 3: Paleo-tectonic maps of the Eastern Mediterranean region at selected time slices at a) 100 Ma, corresponding to the period of subduction initiation at an intra-Neotethyan subduction zone whose remains are widespread on the Anatolian Plateau ophiolites and associated mélange; b) 85 Ma, corresponding to the time window of invasion by roll-back of intra-oceanic subduction zones into the Eastern Mediterranean, culminating in multidirectional ophiolite emplacement onto the Greater Adriatic and Arabian-north African continental margin; c) 65 Ma, corresponding to the end of ophiolite obduction, arrest of subduction in the Eastern Mediterranean Ocean, break-off of the associated slabs, and continuation of the northern originally intra-oceanic subduction zone by continental subduction and nappe stacking of the Greater Adria continent and overlying ophiolites; d) 45 Ma, corresponding to the time period of upper plate extension of the crust that now forms the East Anatolian Plateau, above the Bitlis subduction zone, whilst subduction below the Eurasian margin continues; e) 20 Ma, corresponding to the time window of upper plate shortening in eastern Anatolia, and the thrusting of the Tauride orogen over the Arabian margin; and f) the Present. Maps are based on the kinematic reconstruction of the Mediterranean region of van Hinsbergen et al. (2020). For key to the main units, see Figure 2.

Figure 4. Schematic cross-sectional evolution of subduction in the east Anatolian region since the Cretaceous. The three main stages of the east Anatolian orogen comprise nappe stacking below oceanic lithosphere preserved as ophiolites (100-65 Ma), upper plate extension and exhumation of previously buried portions of the nappe stack (65-25 Ma), shortening and of the extended nappe stack, during which extrusion tectonics gradually developed in the late Neogene (25-0 Ma).

Figure 5. Major active faults and epicenter of earthquakes (Mw ≥ 5) in Eastern Turkey. Focal mechanism solutions are provided by AFAD (Ministry of Interior Disaster and Emergency Management Presidency) and their locations are indicated with red dots with numbers. White dots represent the location of the earthquakes provided by the USGS (United States Geological Survey). The base map utilizes a Digital Elevation Model (DEM) provided by ASTER GDEM, with a horizontal resolution of 1 arc-second.

Figure 6: Simplified kinematic cartoon illustrating that the estimated amount of Anatolian extrusion of 85 km along the North Anatolian Fault since 13 Ma accommodates more than ~65 km of Arabia-Eurasia convergence, ~25%. The remaining >200 km of convergence must have been accommodated by crustal shortening and thickening, uplifting the East Anatolian Plateau.

Figure 7: Paleo-tectonic maps of the East Anatolian Plateau. For clarity, the widespread ophiolite klippen, plutons, and sedimentary cover has been removed from the maps. Time slice at a) 18 Ma, corresponds to the time of onset of thrusting of the Tauride orogen over the Arabian margin; b) 13 Ma, corresponds to the onset of formation of the North Anatolian Fault; c) 5 Ma, corresponds to the onset of formation of the East Anatolian Fault, and d) corresponds to the Present. Maps are based on the kinematic reconstruction of the Mediterranean region of van Hinsbergen et al. (2020). BM = Bitlis Massif; CT = Cyprus Trench; Cy = Cyprus; EAFZ = East Anatolian Fault Zone; GF = Göksün Fault; KB = Kahramanmaraş Basin; MOF = Malatya-Ovacık Fault; NAFZ = North Anatolian Fault Zone; SB = Sivas Basin; SF = Sürgü Fault
For key to the main units, see Figure 2.

References

Akbayram, K., Sorlien, C.C., Okay, A.I., 2016. Evidence for a minimum 52±1km of total offset along the northern branch of the North Anatolian Fault in northwest Turkey. Tectonophysics 668-669, 35-41.

Aktaş, G., Robertson, A., 1984. The Maden Complex, SE Turkey: evolution of a Neotethyan active margin. Geological Society, London, Special Publications 17, 375-402.

Albino, I., Cavazza, W., Zattin, M., Okay, A. I., Adamia, S., Sadradze, N., 2014. Far-field tectonic effects of the Arabia–Eurasia collision and the inception of the North Anatolian Fault system. Geological Magazine 151, 372-379.

Artemieva, I. M., Shulgin, A., 2019. Geodynamics of Anatolia: Lithosphere thermal structure and thickness. Tectonics 38, 4465-4487.

Balkaya, M., Ozden, S., Akyüz, H.S., 2021. Morphometric and Morphotectonic characteristics of Sürgü and Çardak Faults (East Anatolian Fault Zone). Journal of Advanced Research in Natural and Applied Sciences 7, 375-392.

Barazangi, M., Sandvol, E., Seber, D., 2006. Structure and tectonic evolution of the Anatolian plateau in eastern Turkey. Geological Society of America Special Paper 409, 463-473.

Barbot, S., Luo, H., Wang, T., Hamiel, Y., Piatibratova, O., Javed, M.T., Braitenberg, C., Gurbuz, G., 2023. Slip distribution of the February 6, 2023 Mw 7.8 and Mw 7.6, Kahramanmaraş, Turkey earthquake sequence in the East Anatolian Fault Zone. Seismica 2.

Brun, J.P., Sokoutis, D., 2010. 45 m.y. of Aegean crust and mantle flow driven by trench retreat. Geology 38, 815-818.

Buiter, S.J., Govers, R., Wortel, M., 2002. Two-dimensional simulations of surface deformation caused by slab detachment. Tectonophysics 354, 195-210.

Cavazza, W., Cattò, S., Zattin, M., Okay, A.I., Reiners, P., 2018. Thermochronology of the Miocene Arabia-Eurasia collision zone of southeastern Turkey. Geosphere 14, 2277-2293.

Cavazza, W., Gusmeo, T., Zattin, M., Alania, V., Enukidze, O., Corrado, S., Schito, A., 2024. Two-step exhumation of Caucasian intraplate rifts: A proxy of sequential plate-margin collisional orogenies. Geoscience Frontiers 15, 101737.

Cinku, M.C., 2017. Paleomagnetic results from Northeast Anatolia: remagnetization in Late Cretaceous sandstones and tectonic rotation at the Eastern extension of the Izmir–Ankara–Erzincan suture zone. Acta Geophysica 65, 1095-1109.

Cinku, M.C., Heller, F., Ustaömer, T., 2017. New paleomagnetic results from Upper Cretaceous arc-type rocks from the northern and southern branches of the Neotethys ocean in Anatolia. International Journal of Earth Sciences 106, 2575-2592.

Cowgill, E., Forte, A.M., Niemi, N., Avdeev, B., Tye, A., Trexler, C., Javakhishvili, Z., Elashvili, M., Godoladze, T., 2016. Relict basin closure and crustal shortening budgets during continental collision: An example from Caucasus sediment provenance. Tectonics 35, 2918-2947.

Darin, M. H. P. Umhoefer, 2019. Structure and kinematic evolution of the southern Sivas fold-thrust belt, Sivas Basin, Central Anatolia, Turkey. Turkish Journal of Earth Sciences 28, 834-859.

DeMets, C., Iaffaldano, G., Merkouriev, S., 2015. High-resolution Neogene and Quaternary estimates of Nubia-Eurasia-North America Plate motion. Geophysical Journal International 203, 416-427.

DeMets, C., Merkouriev, S., 2016. High-resolution estimates of Nubia–Somalia plate motion since 20 Ma from reconstructions of the Southwest Indian Ridge, Red Sea and Gulf of Aden. Geophysical Journal International 207, 317-332.

Dewey, J., Şengör, A.M.C., 1979. Aegean and surrounding regions: complex multiplate and continuum tectonics in a convergent zone. Geological Society of America Bulletin 90, 84-92.

Duman, T.Y., Elmacı, H., Özalp, S., Kürçer, A., Kara, M., Özdemir, E., Yavuzoğlu, A., Uygun Güldoğan, Ç., 2020. Paleoseismology of the western Sürgü–Misis fault system: east Anatolian Fault, Turkey. Mediterranean Geoscience Reviews 2, 411-437.

Duman, T.Y., Emre, Ö., 2013. The East Anatolian Fault: geometry, segmentation and jog characteristics. Geological Society, London, Special Publications 372, SP372. 314.

Elliott, J. R., Copley, A. C., Holley, R., Scharer, K., Parsons, B., 2013. The 2011 Mw 7.1 van (eastern Turkey) earthquake. Journal of Geophysical Research 118, 1619-1637.

Emre, Ö., Duman, T.Y., Özalp, S., Şaroğlu, F., Olgun, Ş., Elmacı, H., Çan, T., 2018. Active fault database of Turkey. Bulletin of Earthquake Engineering 16, 3229-3275.

Endrun, B., Lebedev, S., Meier, T., Tirel, C., Friederich, W., 2011. Complex layered deformation within the Aegean crust and mantle revealed by seismic anisotropy. Nature Geoscience 4, 203-207.

Faccenna, C., Bellier, O., Martinod, J., Piromallo, C., Regard, V., 2006. Slab detachment beneath eastern Anatolia: A possible cause for the formation of the North Anatolian fault. Earth and Planetary Science Letters 242, 85-97.

Fielding, E.J., Lundgren, P.R., Taymaz, T., Yolsal-Çevikbilen, S., Owen, S.E., 2013. Fault-slip source models for the 2011 M 7.1 Van earthquake in Turkey from SAR interferometry, pixel offset tracking, GPS, and seismic waveform analysis. Seismological Research Letters 84, 579-593.

Forte, A. M., Gutterman, K.R., van Soest, M. C., Gallagher, K., 2022. Building a Young Mountain Range: Insight into the growth of the Greater Caucasus mountains from detrital zircon (U-Th)/He thermochronology and 10Be erosion rates. Tectonics 41, e2021TC006900.

Göğüş, O.H., Pysklywec, R.N., 2008. Mantle lithosphere delamination driving plateau uplift and synconvergent extension in eastern Anatolia. Geology 36, 723-726.

Göğüş, O. H., Pysclywec, R.N., Sengör, A.M.C., Gun, E., 2017. Drip tectonics and the enigmatic uplift of the Central Anatolian Plateau. Nature Communications 8, 1538.

Gülyüz, E., Durak, H., Özkaptan, M., Krijgsman, W., 2020. Paleomagnetic constraints on the early Miocene closure of the southern Neo-Tethys (Van region; East Anatolia): Inferences for the timing of Eurasia- Arabia collision. Global and Planetary Change 185, 103089.

Gürer, D., van Hinsbergen, D.J.J., 2019. Diachronous demise of the Neotethys Ocean as a driver for non-cylindrical orogenesis in Anatolia. Tectonophysics 760, 95-106.

Gürer, D., van Hinsbergen, D.J.J., Matenco, L., Corfu, F., Cascella, A., 2016. Kinematics of a former oceanic plate of the Neotethys revealed by deformation in the Ulukışla basin (Turkey). Tectonics 35, 2385-2416.

Gürer, D., van Hinsbergen, D.J.J., Özkaptan, M., Creton, I., Koymans, M.R., Cascella, A., Langereis, C.G., 2018. Paleomagnetic constraints on the timing and distribution of Cenozoic rotations in Central and Eastern Anatolia. Solid Earth 9, 295-322.

Gusmeo, T., Cavazza, W., Alania, V. M., Enukidze, O. V., Zattin, M., & Corrado, S., 2021. Structural inversion of back-arc basins–The Neogene Adjara-Trialeti fold-and-thrust belt (SW Georgia) as a far-field effect of the Arabia-Eurasia collision. Tectonophysics 803, 228702.

Hafkenscheid, E., Wortel, M.J.R., Spakman, W., 2006. Subduction history of the Tethyan region derived from seismic tomography and tectonic reconstructions. Journal of Geophysical Research 111.

Higgins, M., Schoenbohm, L.M., Brocard, G., Kaymakcı, N., Gosse, J.C., Cosca, M.A., 2015. New kinematic and geochronologic evidence for the Quaternary evolution of the Central Anatolian fault zone (CAFZ). Tectonics 34, 2118-2141.

Hubert-Ferrari, A., King, G., Woerd, J.v.d., Villa, I., Altunel, E., Armijo, R., 2009. Long-term evolution of the North Anatolian Fault: new constraints from its eastern termination. Geological Society, London, Special Publications 311, 133-154.

Hubert-Ferrari, A., Armijo, R., King, G., Meyer, B., Barka, A., 2002. Morphology, displacement, and slip rates along the North Anatolian Fault, Turkey. Journal of Geophysical Research: Solid Earth 107, ETG-9.

Hüsing, S.K., Zachariasse, W.-J., van Hinsbergen, D.J.J., Krijgsman, W., Inceöz, M., Harzhauser, M., Mandic, O., Kroh, A., 2009. Oligocene–Miocene basin evolution in SE Anatolia, Turkey: constraints on the closure of the eastern Tethys gateway. Geological Society, London, Special Publications 311, 107-132.

Huvaz, O., 2009. Comparative petroleum systems analysis of the interior basins of Turkey: Implications for petroleum potential. Marine and Petroleum Geology 26, 1656-1676.

Jaffey, N., Robertson, A.H., 2001. New sedimentological and structural data from the Ecemiş Fault Zone, southern Turkey: implications for its timing and offset and the Cenozoic tectonic escape of Anatolia. Journal of the Geological Society 158, 367-378.

Jolivet, L., Brun, J.-P., 2010. Cenozoic geodynamic evolution of the Aegean. International Journal of Earth Sciences 99, 109-138.

Kapp, P., Guynn, J.H., 2004. Indian punch rifts Tibet. Geology 32.

Karaoğlu, Ö., Selçuk, A.S., Gudmundsson, A., 2017. Tectonic controls on the Karlıova triple junction (Turkey): Implications for tectonic inversion and the initiation of volcanism. Tectonophysics 694, 368-384.

Kaymakcı, N., Inceöz, M., Ertepinar, P., Koç, A., 2010. Late Cretaceous to Recent kinematics of SE Anatolia (Turkey). Geological Society, London, Special Publications 340, 409-435.

Kergaravat, C., Ribes, C., Callot, J.-P., Ringenbach, J.-C., 2017. Tectono-stratigraphic evolution of salt-controlled minibasins in a fold and thrust belt, the Oligo-Miocene central Sivas Basin. Journal of Structural Geology 102, 75-97.

Keskin, M., 2003. Magma generation by slab steepening and breakoff beneath a subduction-accretion complex: An alternative model for collision-related volcanism in Eastern Anatolia, Turkey. Geophysical Research Letters 30.

Ketin, I., 1948. Über die tektonisch-mechanischen Folgerungen aus den grossen anatolischen Erdbeben des letzten Dezenniums. Geologische Rundschau 36, 77-83.

Koç, A., Kaymakcı, N., 2013. Kinematics of Sürgü Fault Zone (Malatya, Turkey): A remote sensing study. Journal of Geodynamics 65, 292-307.

Koçyiğit, A., Beyhan, A., 1998. A new intracontinental transcurrent structure: the Central Anatolian Fault Zone, Turkey. Tectonophysics 284, 317-336.

Koçyiğit, A., Yılmaz, A., Adamia, S., Kuloshvili, S., 2001. Neotectonics of East Anatolian Plateau (Turkey) and Lesser Caucasus: implication for transition from thrusting to strike-slip faulting. Geodinamica Acta 14, 177-195.

Kuşcu, İ., Kuşcu, G.G., Tosdal, R.M., Ulrich, T.D., Friedman, R., 2010. Magmatism in the southeastern Anatolian orogenic belt: transition from arc to post-collisional setting

in an evolving orogen. Geological Society, London, Special Publications 340, 437-460.
Kuşcu, İ., Tosdal, R.M., Gencalioğlu-Kuşcu, G., Friedman, R., Ullrich, T.D., 2013. Late Cretaceous to Middle Eocene magmatism and metallogeny of a portion of the Southeastern Anatolian orogenic belt, East-Central Turkey. Economic Geology 108, 641-666.
Le Pichon, X., Kreemer, C., 2010. The Miocene-to-Present Kinematic Evolution of the Eastern Mediterranean and Middle East and Its Implications for Dynamics. Annual Review of Earth and Planetary Sciences 38, 323-351.
Lefebvre, C., Meijers, M.J.M., Kaymakcı, N., Peynircioğlu, A., Langereis, C.G., van Hinsbergen, D.J.J., 2013. Reconstructing the geometry of central Anatolia during the late Cretaceous: Large-scale Cenozoic rotations and deformation between the Pontides and Taurides. Earth and Planetary Science Letters 366, 83-98.
Legeay, E., Ringenbach, J.-C., Kergaravat, C., Pichat, A., Mohn, G., Vergés, J., Kavak, K.S., Callot, J.-P., 2019. Structure and kinematics of the Central Sivas Basin (Turkey): Salt deposition and tectonics in an evolving fold-and-thrust belt. Geological Society, London, Special Publications 490, SP490-2019-2092.
Li, S., Advokaat, E.L., van Hinsbergen, D.J.J., Koymans, M., Deng, C., Zhu, R., 2017. Paleomagnetic constraints on the Mesozoic-Cenozoic paleolatitudinal and rotational history of Indochina and South China: Review and updated kinematic reconstruction. Earth-Science Reviews 171, 58-77.
Liu, C., Lay, T., Wang, R., Taymaz, T., Xie, Z., Xiong, X., Irmak, T.S., Kahraman, M., Erman, C., 2023. Complex multi-fault rupture and triggering during the 2023 earthquake doublet in southeastern Turkiye. Nat Commun 14, 5564.
Maffione, M., van Hinsbergen, D.J.J., de Gelder, G.I.N.O., van der Goes, F.C., Morris, A., 2017. Kinematics of Late Cretaceous subduction initiation in the Neo-Tethys Ocean reconstructed from ophiolites of Turkey, Cyprus, and Syria. Journal of Geophysical Research: Solid Earth 122, 3953-3976.
Mann, P., Taylor, F., Edwards, R.L., Ku, T.-L., 1995. Actively evolving microplate formation by oblique collision and sideways motion along strike-slip faults: An example from the northeastern Caribbean plate margin. Tectonophysics 246, 1-69.
McKenzie, D.P., Parker, R.L., 1967. The North Pacific: an example of tectonics on a sphere. Nature 216, 1276-1280.
McPhee, P.J., Altıner, D., van Hinsbergen, D.J.J., 2018. First Balanced Cross Section Across the Taurides Fold-Thrust Belt: Geological Constraints on the Subduction History of the Antalya Slab in Southern Anatolia. Tectonics.
McPhee, P.J., Koç, A., van Hinsbergen, D.J.J., 2022. Preparing the ground for plateau growth: Late Neogene Central Anatolian uplift in the context of orogenic and geodynamic evolution since the Cretaceous. Tectonophysics 822, 229131.
McPhee, P.J., van Hinsbergen, D.J.J., 2019. Tectonic reconstruction of Cyprus reveals Late Miocene continental collision between Africa and Anatolia. Gondwana Research 68, 158-173.
Melgar, D., Taymaz, T., Ganas, A., Crowell, B.W., Öcalan, T., Kahraman, M., Tsironi, V., Yolsal-Çevikbil, S., Valkaniotis, S., Irmak, T.S., 2023. Sub-and super-shear ruptures during the 2023 Mw 7.8 and Mw 7.6 earthquake doublet in SE Türkiye. Seismica 2, 1-10.
Memiş, C., Göğüş, O.H., Uluocak, E.Ş., Pysklywec, R., Keskin, M., Şengör, A.C., Topuz, G., 2020. Long wavelength progressive plateau uplift in Eastern Anatolia since 20 Ma:

implications for the role of slab peel-Back and Break-off. Geochemistry, Geophysics, Geosystems 21, e2019GC008726.
Molin, P., Sembroni, A., Ballato, P., Faccenna, C., 2023. The uplift of an early stage collisional plateau unraveled by fluvial network analysis and river longitudinal profile inversion: The case of the Eastern Anatolian Plateau. Tectonics 42.
Molnar, P., Tapponnier, P., 1975. Cenozoic tectonics of Asia: effects of a continental collision. science 189, 419-426.
Mueller, M., Licht, A., Campbell, C., Ocakoğlu, F., Taylor, M., Burch, L., Ugrai, T., Kaya, M., Kurtoğlu, B., Coster, P., 2019. Collision chronology along the İzmir-Ankara-Erzincan suture zone: Insights from the Sarıcakaya Basin, western Anatolia. Tectonics 38, 3652-3674.
Muñoz, J.A., 1992. Evolution of a continental collision belt: ECORS-Pyrenees crustal balanced cross-section, in: McClay, K.R. (Ed.), Thrust Tectonics. Springer Netherlands, Dordrecht, pp. 235-246.
Nikogosian, I.K., Bracco Gartner, A.J., Mason, P.R., van Hinsbergen, D.J.J., Kuiper, K.F., Kirscher, U., Matveev, S., Grigoryan, A., Grigoryan, E., Israyelyan, A., 2023. The South Armenian Block: Gondwanan origin and Tethyan evolution in space and time. Gondwana Research 121, 168-195.
Nuriel, P., Craddock, J., Kylander-Clark, A.R., Uysal, I.T., Karabacak, V., Dirik, R.K., Hacker, B.R., Weinberger, R., 2019. Reactivation history of the North Anatolian fault zone based on calcite age-strain analyses. Geology 47, 465-469.
Oberhänsli, R., Candan, O., Wilke, F., 2010. Geochronological Evidence of Pan-African Eclogites from the Central Menderes Massif, Turkey. Turkish Journal of Earth Sciences 19, 431-447.
Oberhänsli, R., Koralay, E., Candan, O., Pourteau, A., Bousquet, R., 2014. Late Cretaceous eclogitic high-pressure relics in the Bitlis Massif. Geodinamica Acta 26, 175-190.
Ocakoğlu, F., Hakyemez, A., Açıkalın, S., Özkan Altıner, S., Büyükmeriç, Y., Licht, A., Demircan, H., Şafak, Ü., Yıldız, A., Yılmaz, İ.Ö., 2019. Chronology of subduction and collision along the İzmir-Ankara suture in Western Anatolia: records from the Central Sakarya Basin. International Geology Review 61, 1244-1269.
Okay, A.I., Zattin, M., Cavazza, W., 2010. Apatite fission-track data for the Miocene Arabia-Eurasia collision. Geology 38, 35-38.
Philippon, M., Brun, J.-P., Gueydan, F., Sokoutis, D., 2014. The interaction between Aegean back-arc extension and Anatolia escape since Middle Miocene. Tectonophysics 631, 176-188.
Racano, S., Schildgen, T., Ballato, P., Yıldırım, C., Wittmann, H., 2023. Rock-uplift history of the Central Pontides from river-profile inversions and implications for development of the North Anatolian Fault. Earth and Planetary Science Letters 616, 118231.
Reilinger, R., McClusky, S., Vernant, P., Lawrence, S., Ergintav, S., Cakmak, R., Ozener, H., Kadirov, F., Guliev, I., Stepanyan, R., Nadariya, M., Hahubia, G., Mahmoud, S., Sakr, K., ArRajehi, A., Paradissis, D., Al-Aydrus, A., Prilepin, M., Guseva, T., Evren, E., Dmitrotsa, A., Filikov, S.V., Gomez, F., Al-Ghazzi, R., Karam, G., 2006. GPS constraints on continental deformation in the Africa-Arabia-Eurasia continental collision zone and implications for the dynamics of plate interactions. Journal of Geophysical Research: Solid Earth 111, n/a-n/a.
Robertson, A., Parlak, O., Rizaoğlu, T., Ünlügenç, Ü., İnan, N., Tasli, K., Ustaömer, T., 2007. Tectonic evolution of the South Tethyan ocean: evidence from the Eastern Taurus

Mountains (Elaziğ region, SE Turkey). Geological Society, London, Special Publications 272, 231-270.

Sakellariou, D., Tsampouraki-Kraounaki, K., 2019. Plio-Quaternary extension and strike-slip tectonics in the Aegean, Transform plate boundaries and fracture zones. Elsevier, pp. 339-374.

Sançar, T., Zabcı, C., Akcar, N., Karabacak, V., Yeşilyurt, S., Yazıcı, M., Akyüz, H.S., Önal, A.Ö., Ivy-Ochs, S., Christl, M., 2020. Geodynamic importance of the strike-slip faults at the eastern part of the Anatolian Scholle: Inferences from the uplift and slip rate of the Malatya Fault (Malatya-Ovacık Fault Zone, eastern Turkey). Journal of Asian earth sciences 188, 104091.

Sançar, T., Zabcı, C., Akyüz, H.S., Sunal, G., Villa, I.M., 2015. Distributed transpressive continental deformation: the Varto Fault Zone, eastern Turkey. Tectonophysics 661, 99-111.

Sançar, T., Zabcı, C., Karabacak, V., Yazıcı, M., Akyüz, H.S., 2019. Geometry and Paleoseismology of the Malatya Fault (Malatya-Ovacık Fault Zone), Eastern Turkey: Implications for intraplate deformation of the Anatolian Scholle. Journal of Seismology 23, 319-340.

Saroğlu, F., 1992. The east Anatolian fault zone of Turkey. Ann. Tectonicae, 99-125.

Schepers, G., van Hinsbergen, D.J.J., Spakman, W., Kosters, M.E., Boschman, L.M., McQuarrie, N., 2017. South-American plate advance and forced Andean trench retreat as drivers for transient flat subduction episodes. Nat Commun 8, 15249.

Schmid, S. M., Bernoulli, D., Fügenschuh, B., Georgiev, N., Kounov, A., Matenco, L., Oberhänsli, R., Pleuger, J., Schefer, S., Schuster, B., Tomljenovic, B., Ustaszewski, K., van Hinsbergen, D.J.J., 2020. Tectonic units of the Alpine collision zone between Eastern Alps and Western Turkey. Gondwana Research 78, 308-374.

Şenel, M., 2002. Geological Map of Turkey in 1/500.000 scale. Publication of Mineral Research and Exploration Directorate of Turkey (MTA), Ankara.

Sengör, A., 1979. The North Anatolian transform fault: its age, offset and tectonic significance. Journal of the Geological Society 136, 269-282.

Şengör, A.M.C., Özeren, M., Genç, T., Zor, E., 2003. East Anatolian High Plateau as a mantle-supported, north-south shortened domal structure. Geophysical Research Letters 30, 8050.

Şengör, A.M.C., Özeren, M.S., Keskin, M., Sakınç, M., Özbakır, A.D., Kayan, İ., 2008. Eastern Turkish high plateau as a small Turkic-type orogen: Implications for post-collisional crust-forming processes in Turkic-type orogens. Earth-Science Reviews 90, 1-48.

Şengör, A.M.C., Tüysüz, O., İmren, C., Sakınç, M., Eyidoğan, H., Görür, N., Le Pichon, X., Rangin, C., 2005. The North Anatolian Fault: A New Look. Annual Review of Earth and Planetary Sciences 33, 37-112.

Şengör, A.M.C., Yılmaz, Y., 1981. Tethyan evolution of Turkey: A plate tectonic approach. Tectonophysics 75, 181-241.

Simão, N., Nalbant, S.S., Sunbul, F., Mutlu, A.K., 2016. Central and eastern Anatolian crustal deformation rate and velocity fields derived from GPS and earthquake data. Earth and Planetary Science Letters 433, 89-98.

Sosson, M., Rolland, Y., Müller, C., Danelian, T., Melkonyan, R., Kekelia, S., Adamia, S., Babazadeh, V., Kangarli, T., Avagyan, A., 2010. Subductions, obduction and collision in the Lesser Caucasus (Armenia, Azerbaijan, Georgia), new insights. Geological Society, London, Special Publications 340, 329-352.

Stampfli, G. M., C. Hochard, 2009. Plate tectonics of the Alpine realm. Geological Society, London, Special Publications 327, 89-111.

Sternai, P., Jolivet, L., Menant, A., Gerya, T., 2014. Driving the upper plate surface deformation by slab rollback and mantle flow. Earth and Planetary Science Letters 405, 110-118.

Tan, O., Tapirdamaz, M.C., Yörük, A., 2008. The earthquake catalogues for Turkey. Turkish Journal of Earth Sciences 17, 405-418.

Tarı, U., Tüysüz, O., Can Genç, Ş., İmren, C., Blackwell, B.A., Lom, N., Tekeşin, Ö., Üsküplü, S., Erel, L., Altıok, S., 2013. The geology and morphology of the Antakya Graben between the Amik Triple Junction and the Cyprus Arc. Geodinamica Acta 26, 27-55.

Topuz, G., Candan, O., Zack, T., Yılmaz, A., 2017. East Anatolian plateau constructed over a continental basement: No evidence for the East Anatolian accretionary complex. Geology 45, 791-794.

Trexler, C. C., Cowgill, E., Spencer, J. Q., Godoladze, T., 2020. Rate of active shortening across the southern thrust front of the Greater Caucasus in western Georgia from kinematic modeling of folded river terraces above a listric thrust. Earth and Planetary Science Letters 544, 116362.

Şengül Uluocak, E., Pysklywec, R., Göğüş, O. H., 2016. Present-day dynamic and residual topography in Central Anatolia. Geophysical Journal International 206, 1515-1525.

van der Boon, A., van Hinsbergen, D.J.J., Rezaeian, M., Gürer, D., Honarmand, M., Pastor-Galán, D., Krijgsman, W., Langereis, C.G., 2018. Quantifying Arabia–Eurasia convergence accommodated in the Greater Caucasus by paleomagnetic reconstruction. Earth and Planetary Science Letters 482, 454-469.

van Hinsbergen, D.J.J., 2022. Indian Plate paleogeography, subduction, and horizontal underthrusting below Tibet: paradoxes, controversies, and opportunities. National Science Review 9, nwac074.

van Hinsbergen, D.J.J., Hafkenscheid, E., Spakman, W., Meulenkamp, J.E., Wortel, R., 2005. Nappe stacking resulting from subduction of oceanic and continental lithosphere below Greece. Geology 33.

van Hinsbergen, D.J.J., Schmid, S.M., 2012. Map view restoration of Aegean-West Anatolian accretion and extension since the Eocene. Tectonics 31, n/a-n/a.

van Hinsbergen, D.J.J., Schouten, T.L.A., 2021. Deciphering paleogeography from orogenic architecture: constructing orogens in a future supercontinent as thought experiment. American Journal of Science 321, 955-1031.

van Hinsbergen, D.J.J., Torsvik, T., Schmid, S.M., Matenco, L., Maffione, M., Vissers, R.L.M., Gürer, D., Spakman, W., 2020. Orogenic architecture of the Mediterranean region and kinematic reconstruction of its tectonic evolution since the Triassic. Gondwana Research 81, 79-229.

van Hinsbergen, D.J.J., van der Meer, D.G., Zachariasse, W.J., Meulenkamp, J.E., 2006. Deformation of western Greece during Neogene clockwise rotation and collision with Apulia. International Journal of Earth Sciences 95, 463-490.

Vincent, S.J., Morton, A.C., Carter, A., Gibbs, S., Barabadze, T.G., 2007. Oligocene uplift of the Western Greater Caucasus: an effect of initial Arabia–Eurasia collision. Terra Nova 19, 160-166.

Westaway, R., 2004. Kinematic consistency between the Dead Sea Fault Zone and the Neogene and Quaternary left-lateral faulting in SE Turkey. Tectonophysics 391, 203-237.

Westaway, R., Arger, J., 2001. Kinematics of the Malatya–Ovacik fault zone. Geodinamica Acta 14, 103-131.

Whitney, D.L., Delph, J.R., Thomson, S.N., Beck, S.L., Brocard, G.Y., Cosca, M.A., Darin, M.H., Kaymakcı, N., Meijers, M.J., Okay, A.I., 2023. Breaking plates: Creation of the East Anatolian fault, the Anatolian plate, and a tectonic escape system. Geology.

Yılmaz, O., Michel, R., Vialette, Y., Bonhomme, M., 1981. Réinterprétation des données isotopiques Rb-Sr obtenues sur les métamorphites de la partie méridionale du massif de Bitlis (Turquie). Sciences Géologiques, bulletins et mémoires 34, 59-73.

Yılmaz, A., Yılmaz, H., Kaya, C., Boztug, D., 2010. The nature of the crustal structure of the Eastern Anatolian Plateau, Turkey. Geodinamica Acta 23, 167-183.

Yılmaz, Y., Yiğitbaş, E., Genç, Ş. C., 1993. Ophiolitic and metamorphic assemblages of southeast Anatolia and their significance in the geological evolution of the orogenic belt. Tectonics 12, 1280-1297.

Yılmaz, C., 1994. Evolution of the Munzur Carbonate Platform during the Mesozoic, Middle-Eastern Anatolia (Turkey). Géologie Méditerranéenne 21, 195-196.

Yönlü, Ö., Altunel, E., Karabacak, V., Akyüz, H.S., 2013. Evolution of the Gölbaşı basin and its implications for the long-term offset on the East Anatolian Fault Zone, Turkey. Journal of Geodynamics 65, 272-281.

Yusufoğlu, H., 2013. An intramontane pull-apart basin in tectonic escape deformation: Elbistan Basin, Eastern Taurides, Turkey. Journal of Geodynamics 65, 308-329.

Zhang, Y., Tang, X., Liu, D., Taymaz, T., Eken, T., Guo, R., Zheng, Y., Wang, J., Sun, H., 2023. Geometric controls on cascading rupture of the 2023 Kahramanmaraş earthquake doublet. Nature Geoscience, 1-7.

Zor, E., Sandvol, E., Gürbüz, C., Türkelli, N., Seber, D., Barazangi, M., 2003. The crustal structure of the East Anatolian plateau (Turkey) from receiver functions. Geophysical Research Letters 30.

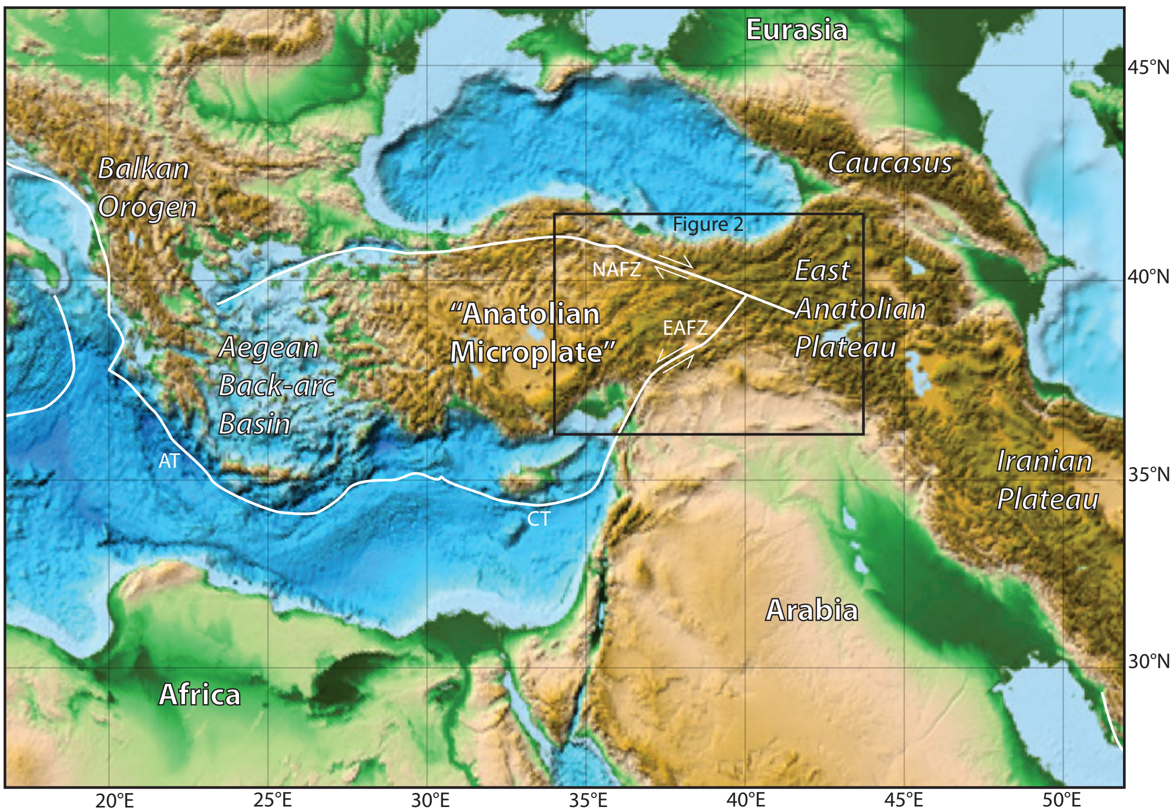

Eurasia
Balkan Orogen
Caucasus
Figure 2
NAFZ
East Anatolian Plateau
"Anatolian Microplate"
EAFZ
Aegean Back-arc Basin
AT
CT
Iranian Plateau
Arabia
Africa
45°N
40°N
35°N
30°N
20°E
25°E
30°E
35°E
40°E
45°E
50°E

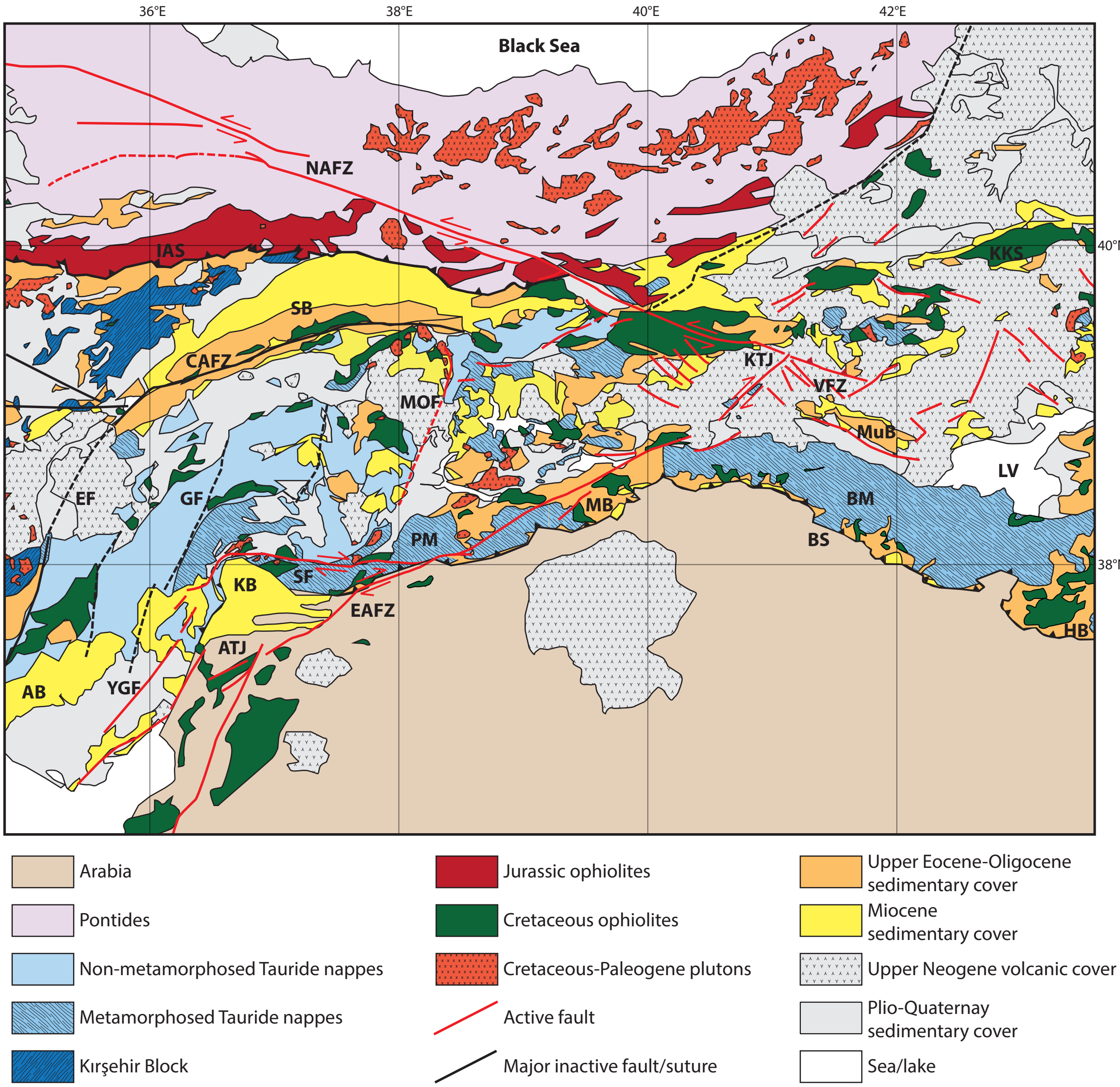
36°E
38°E
40°E
42°E
40°N
38°N
Black Sea
NAFZ
IAS
SB
CAFZ
MOF
KTJ
VFZ
KKS
MuB
LV
EF
GF
PM
MB
BM
BS
KB
SF
EAFZ
ATJ
AB
YGF
HB
Arabia
Pontides
Non-metamorphosed Tauride nappes
Metamorphosed Tauride nappes
Kırşehir Block
Jurassic ophiolites
Cretaceous ophiolites
Cretaceous-Paleogene plutons
Active fault
Major inactive fault/suture
Upper Eocene-Oligocene sedimentary cover
Miocene sedimentary cover
Upper Neogene volcanic cover
Plio-Quaternay sedimentary cover
Sea/lake

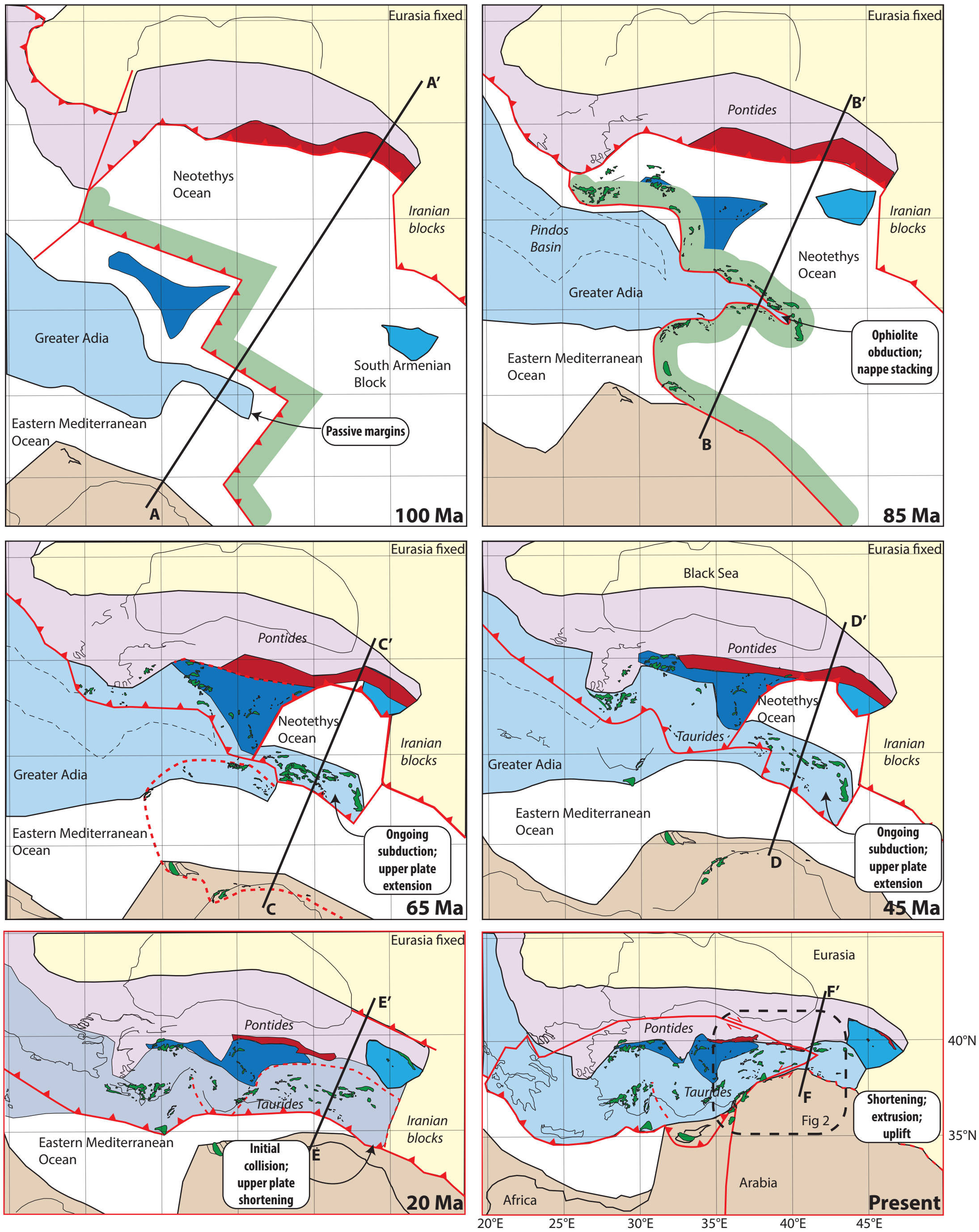

Eurasia fixed
A′
Neotethys Ocean
Iranian blocks
Greater Adia
South Armenian Block
Eastern Mediterranean Ocean
Passive margins
A
100 Ma
Eurasia fixed
Pontides
B′
Iranian blocks
Pindos Basin
Greater Adia
Neotethys Ocean
Eastern Mediterranean Ocean
Ophiolite obduction; nappe stacking
B
85 Ma
Eurasia fixed
Pontides
C′
Neotethys Ocean
Iranian blocks
Greater Adia
Eastern Mediterranean Ocean
Ongoing subduction; upper plate extension
C
65 Ma
Eurasia fixed
Black Sea
D′
Pontides
Neotethys Ocean
Taurides
Iranian blocks
Greater Adia
Eastern Mediterranean Ocean
Ongoing subduction; upper plate extension
D
45 Ma
Eurasia fixed
E′
Pontides
Taurides
Iranian blocks
Eastern Mediterranean Ocean
Initial collision; upper plate shortening
E
20 Ma
Eurasia
F′
Pontides
Taurides
F
Fig 2
Shortening; extrusion; uplift
40°N
35°N
Arabia
Africa
Present
20°E
25°E
30°E
35°E
40°E
45°E

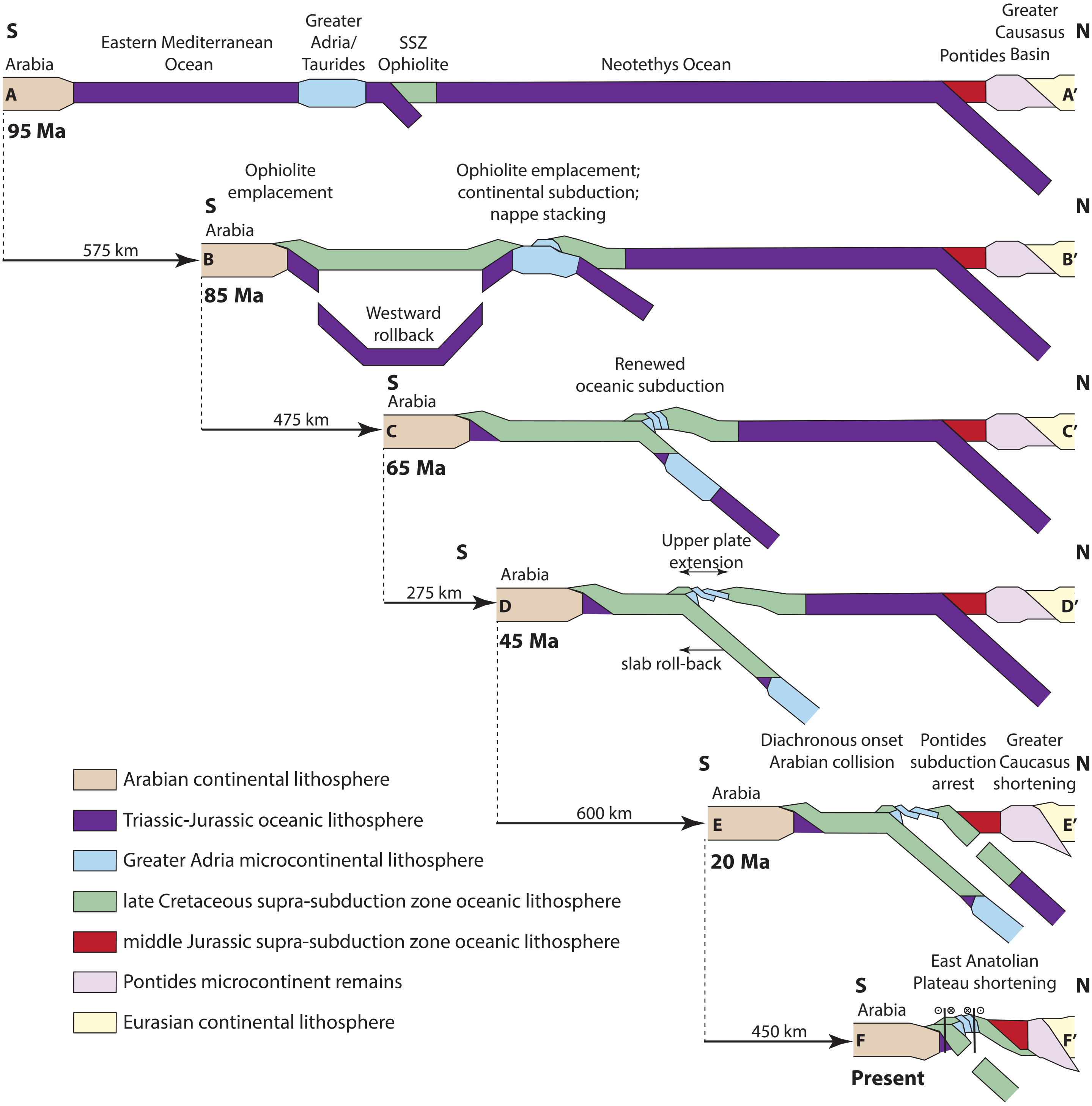
S
Arabia
Eastern Mediterranean Ocean
Greater Adria/ Taurides
SSZ Ophiolite
Neotethys Ocean
Greater Causasus
Pontides Basin
N
A
A'
95 Ma
575 km
S
Arabia
Ophiolite emplacement
Ophiolite emplacement; continental subduction; nappe stacking
N
B
B'
85 Ma
Westward rollback
475 km
S
Arabia
Renewed oceanic subduction
N
C
C'
65 Ma
275 km
S
Arabia
Upper plate extension
N
D
D'
45 Ma
slab roll-back
600 km
S
Arabia
Diachronous onset Arabian collision
Pontides subduction arrest
Greater Caucasus shortening
N
E
E'
20 Ma
450 km
S
Arabia
East Anatolian Plateau shortening
N
F
F'
Present
Arabian continental lithosphere
Triassic-Jurassic oceanic lithosphere
Greater Adria microcontinental lithosphere
late Cretaceous supra-subduction zone oceanic lithosphere
middle Jurassic supra-subduction zone oceanic lithosphere
Pontides microcontinent remains
Eurasian continental lithosphere

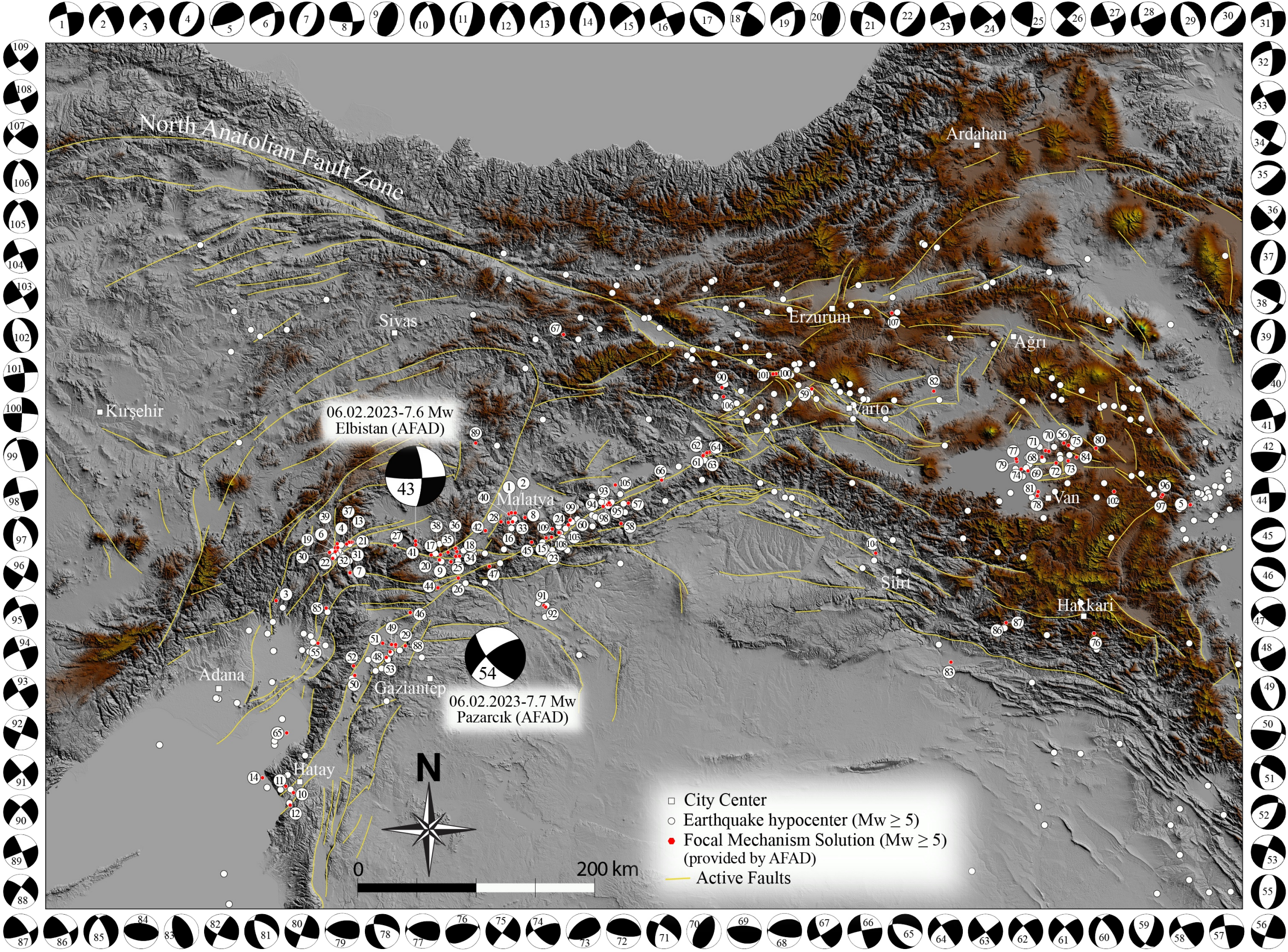
North Anatolian Fault Zone
Ardahan
Erzurum
Ağrı
Sivas
Kırşehir
Varto
Malatya
Van
Siirt
Hakkari
Adana
Gaziantep
Hatay
06.02.2023-7.6 Mw
Elbistan (AFAD)
06.02.2023-7.7 Mw
Pazarcık (AFAD)
N
0
200 km
City Center
Earthquake hypocenter (Mw ≥ 5)
Focal Mechanism Solution (Mw ≥ 5)
(provided by AFAD)
Active Faults

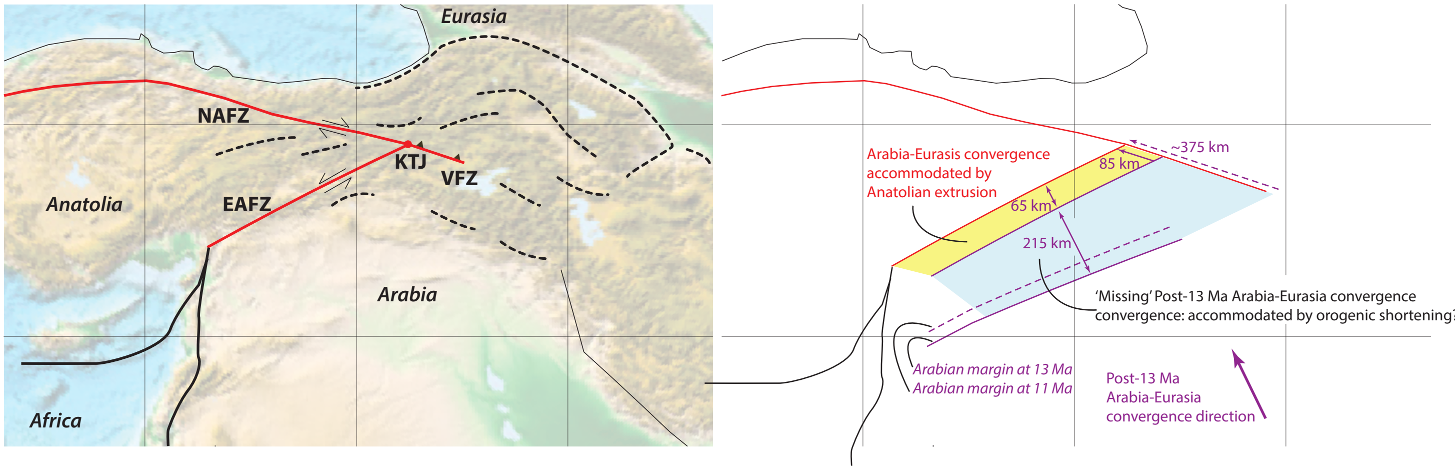

Eurasia
NAFZ
KTJ
VFZ
Anatolia
EAFZ
Arabia
Africa
~375 km
Arabia-Eurasis convergence
accommodated by
Anatolian extrusion
85 km
65 km
215 km
'Missing' Post-13 Ma Arabia-Eurasia convergence
convergence: accommodated by orogenic shortening?
Arabian margin at 13 Ma
Arabian margin at 11 Ma
Post-13 Ma
Arabia-Eurasia
convergence direction

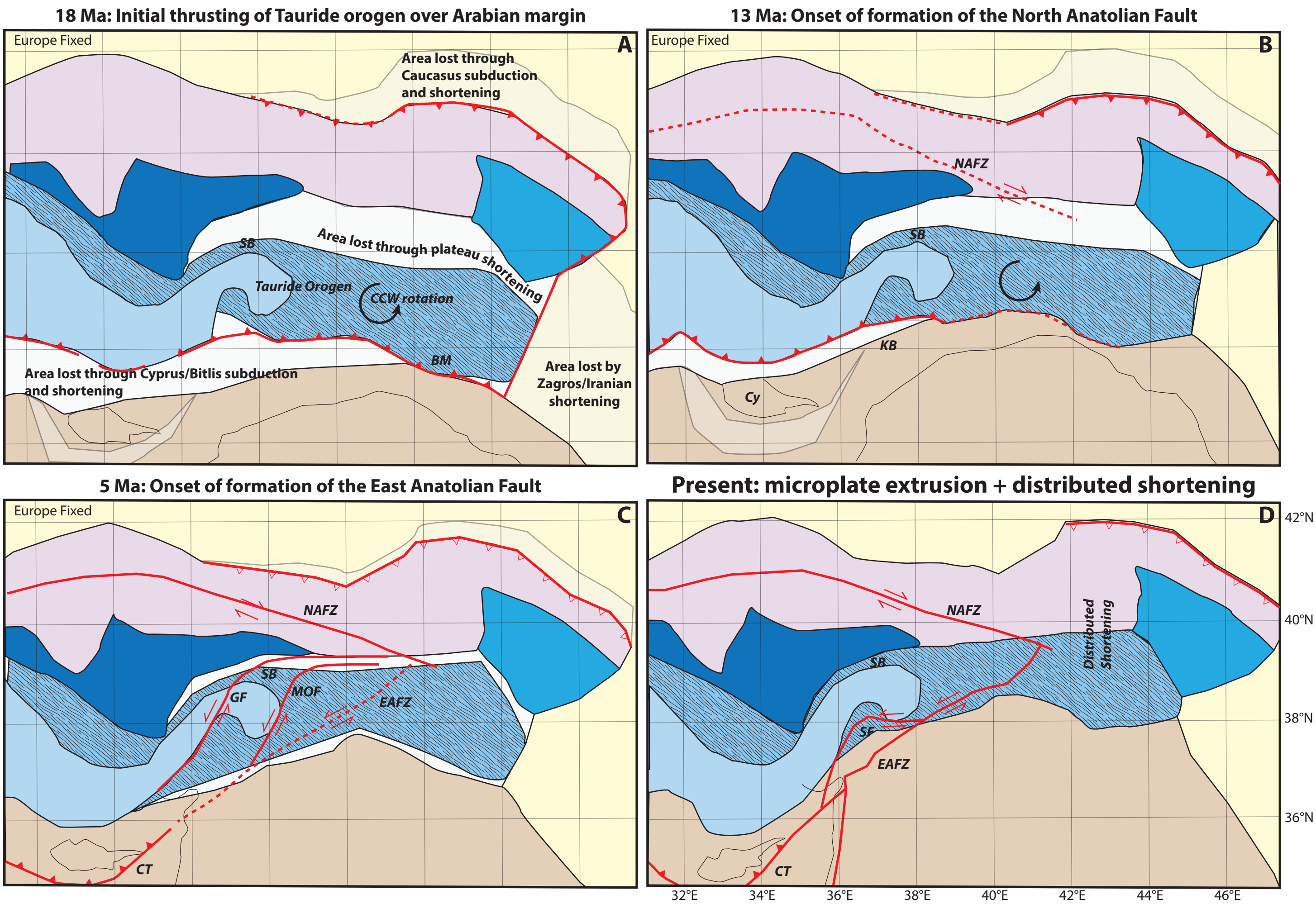
18 Ma: Initial thrusting of Tauride orogen over Arabian margin
Europe Fixed
A
Area lost through Caucasus subduction and shortening
SB
Area lost through plateau shortening
Tauride Orogen
CCW rotation
BM
Area lost through Cyprus/Bitlis subduction and shortening
Area lost by Zagros/Iranian shortening
13 Ma: Onset of formation of the North Anatolian Fault
Europe Fixed
B
NAFZ
SB
KB
Cy
5 Ma: Onset of formation of the East Anatolian Fault
Europe Fixed
C
NAFZ
SB
GF
MOF
EAFZ
CT
Present: microplate extrusion + distributed shortening
D
NAFZ
SB
Distributed Shortening
SF
EAFZ
CT
42°N
40°N
38°N
36°N
32°E
34°E
36°E
38°E
40°E
42°E
44°E
46°E